

# The Osceola Mudflow from Mount Rainier: Sedimentology and hazard implications of a huge clay-rich debris flow

James W. Vallance }  
Kevin M. Scott } U.S. Geological Survey, 5400 MacArthur Boulevard, Vancouver, Washington 98661

## ABSTRACT

The 3.8 km<sup>3</sup> Osceola Mudflow began as a water-saturated avalanche during phreatomagmatic eruptions at the summit of Mount Rainier about 5600 years ago. It filled valleys of the White River system north and northeast of Mount Rainier to depths of more than 100 m, flowed northward and westward more than 120 km, covered more than 200 km<sup>2</sup> of the Puget Sound lowland, and extended into Puget Sound. The lahar had a velocity of  $\approx 19$  m/s and peak discharge of  $\approx 2.5 \times 10^6$  m<sup>3</sup>/s, 40 to 50 km downstream, and was hydraulically dammed behind a constriction. It was coeval with the Paradise lahar, which flowed down the south side of Mount Rainier, and was probably related to it genetically.

Osceola Mudflow deposits comprise three facies. The axial facies forms normally graded deposits 1.5 to 25 m thick in lowlands and valley bottoms and thinner ungraded deposits in lowlands; the valley-side facies forms ungraded deposits 0.3 to 2 m thick that drape valley slopes; and the hummocky facies, interpreted before as a separate (Greenwater) lahar, forms 2–10-m-thick deposits dotted with numerous hummocks up to 20 m high and 60 m in plan.

Deposits show progressive downstream improvement in sorting, increase in sand and gravel, and decrease in clay. These downstream progressions are caused by incorporation (bulking) of better sorted gravel and sand. Normally graded axial deposits show similar trends from top to bottom because of bulking. The coarse-grained basal deposits in valley bottoms are similar to deposits near inundation limits. Normal grading in deposits is best explained by incremental aggradation of a flow wave, coarser grained at its front than at its tail.

The Osceola Mudflow transformed completely from debris avalanche to clay-rich (cohesive) lahar within 2 km of its source because of the presence within the preavalanche mass of large volumes of pore water and abundant weak hydrothermally altered rock. A survey of cohesive lahars suggests that the amount of hydrothermally altered rock in the preavalanche mass determines whether a debris avalanche will transform into a cohesive debris flow or remain a largely unsaturated debris avalanche. The distinction among cohesive lahar, noncohesive lahar, and debris avalanche is important in hazard assessment because cohesive lahars spread much more widely than noncohesive lahars that travel similar distances, and travel farther and spread more widely

than debris avalanches of similar volume. The Osceola Mudflow is documented here as an example of a cohesive debris flow of huge size that can be used as a model for hazard analysis of similar flows.

## INTRODUCTION

The Osceola Mudflow began as an avalanche or a series of avalanches at the summit of Mount Rainier in west-central Washington State about 5600 yr (4800 radiocarbon yr) B.P. (Crandell, 1971). It is the largest of several catastrophic lahars that swept down the White River drainage during Holocene time and one of the world's largest lahars (Fig. 1).

The distribution of the Osceola Mudflow, many of its features, and the character of the eruptions that produced it were investigated in the seminal work of Crandell and Mullineaux on the surficial geology of Mount Rainier and vicinity (Crandell and Waldron, 1956; Crandell, 1963a, 1963b, 1969, 1971; Mullineaux, 1965a, 1965b, 1974). Many of the ideas presented here are naturally similar to those of Crandell and Mullineaux; however, some of our conclusions differ from their conclusions, and our results require a revision of the events that led to and culminated in the Osceola Mudflow. In particular, we investigate the stratigraphic relationships of tephra units to the Osceola Mudflow, show that all of these units probably were generated during a single phreatomagmatic eruptive episode, and infer that the eruption involved laterally directed explosions. We simplify the inferred pre-Osceola sequence by showing that the Paradise and Greenwater lahars, thought by Crandell (1971) to predate the Osceola Mudflow, are contemporaneous and, specifically, that the Greenwater lahar is actually a hummock-rich facies of the Osceola.

At Mount St. Helens after 1980, detailed stratigraphic and sedimentological study of clay-poor lahars illustrated the facies gradations from top to bottom of outcrops, from valley bottom to inundation limit, and with distance downstream (Scott, 1988). Pierson and Scott (1985) and Scott (1988) showed how the lahars developed from water floods that incorporated sediment by erosion and how they evolved downstream to more dilute (hyperconcentrated) flow. There is as yet no similarly detailed study of a clay-rich avalanche-induced lahar like the Osceola Mudflow. We discuss the facies changes, sedimentology, and inferred behavior of the Osceola Mudflow, show how these characteristics differ from those of typical clay-poor lahars, and suggest that they are typical of huge clay-rich lahars. We examine lateral, longitudinal, and vertical gradations in deposits of the Mudflow and make detailed observations of changes in the character of deposits between lowlying areas and inundation limits in order to infer its behavior. We thereby infer that the Osceola Mudflow was most erosive during waxing and peak flow, and that it progressively incorporated sediment as it

\*Present address: Department of Civil Engineering and Applied Mechanics, McGill University, 817 Sherbrooke Street West, Montréal, Québec H3A 2K6, Canada. E-mail address: james@fuego.civil.mcgill.ca

Data Repository item 9714 contains additional material related to this article.

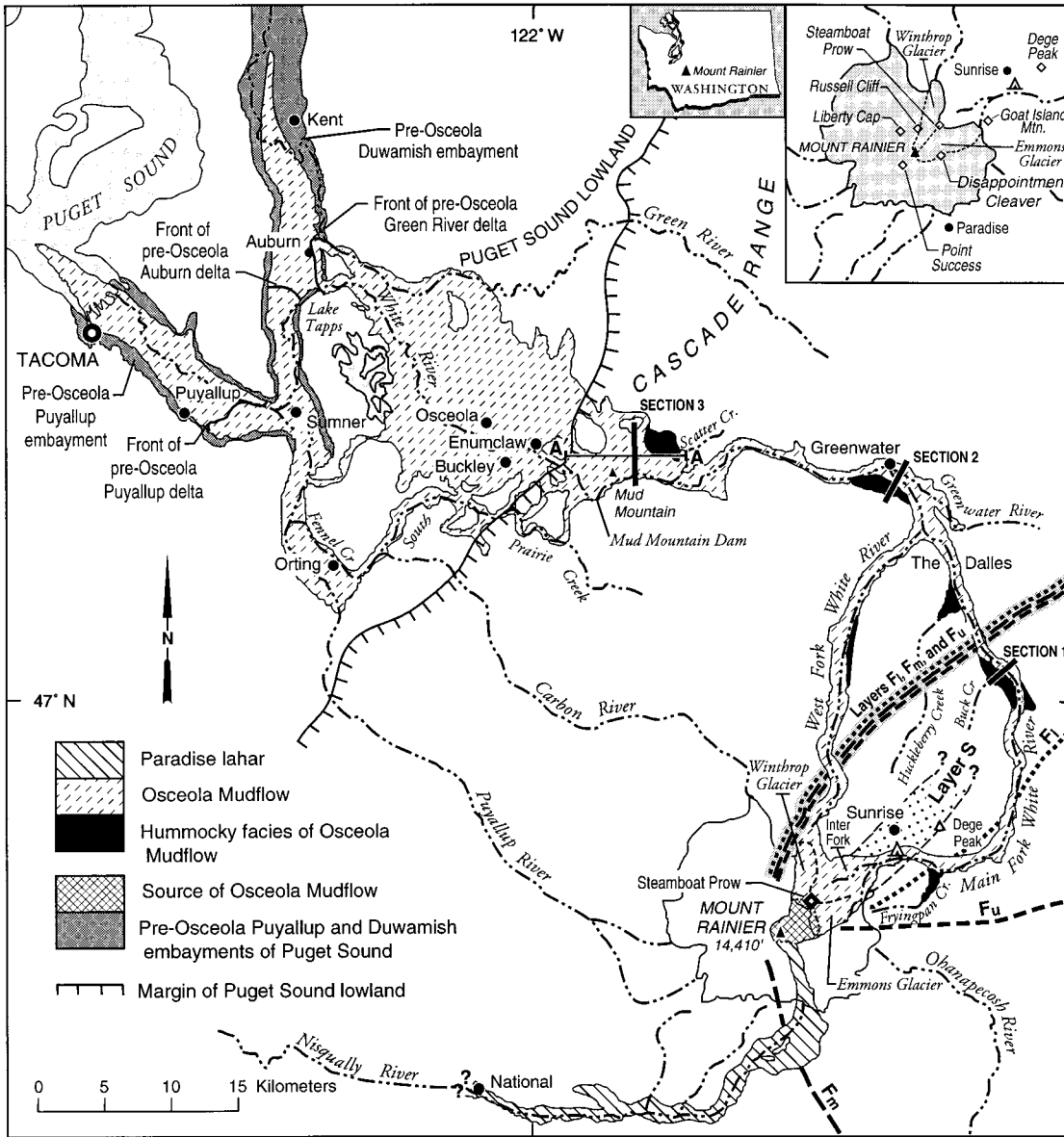


Figure 1. Map showing distribution of Osceola Mudflow and Paradise lahar (modified from Crandell, 1971, plate 3). Distribution of Osceola Mudflow in subsurface from Dragovich et al. (1994). Distributions of tephra layers F and S (Mullineaux, 1974) shown near Mount Rainier. Sections 1, 2, 3, and A-A' shown in Figure 7.

moved down valley. On the basis of facies and sedimentological variations, we suggest that the normal grading common in low-lying deposits is best explained by incremental deposition of a debris wave that is coarser and better sorted near its front than at its tail.

This study is a part of a more comprehensive effort to reevaluate debris flows and their hazards at Mount Rainier (Scott et al., 1995; Scott and Vallance, 1995). A growing body of evidence suggests that there is a complete gradation between sector-collapse-induced debris avalanches and lahars at volcanoes (Neall and Alloway, 1986; Palmer et al., 1991; Carrasco-Núñez et al., 1993; Vallance, 1994a, 1994b; Scott et al., 1995). We discuss the gradation between sector-collapse-induced debris avalanches and huge clay-rich lahars and its significance with respect to hazard appraisal.

**TERMINOLOGY AND RELATED DISCUSSION**

Debris flow is a term used here to indicate any flowing mixture of debris and water having sediment concentration greater than 60% by volume or 80% by weight. Flows having higher water contents, so high that they pos-

sess fluvial characteristics yet carry very high sediment loads, are termed hyperconcentrated flows; depth-integrated sediment concentrations between 20 and 60 vol% or 40 and 80 wt% characterize such flows (Beverage and Culbertson, 1964). We use lahar for a debris flow originating at a volcano and lahar-runout flow for a downstream transformation from debris flow to hyperconcentrated stream flow. We refer to lahar and lahar-runout deposits as lahars and lahar runouts where the meaning is clear. Mudflow, in the sense of a debris flow having a greater than 50% sand-, silt-, and clay-size solid fraction (Crandell, 1971; Varnes, 1978), is not used in this paper, and the term is used only in the formation name, Osceola Mudflow.

A more significant criterion for distinguishing among debris flows is the clay fraction. We empirically separate cohesive debris from noncohesive debris by the ratio of clay to total sand, silt, and clay (sand-, silt-, and clay-size fractions) and suggest that a ratio of about 0.05 divides cohesive and noncohesive debris flows (Fig. 2). In using this terminology, we intend to distinguish between noncohesive flows, which commonly begin as water floods that incorporate sediment through erosion then transform down-

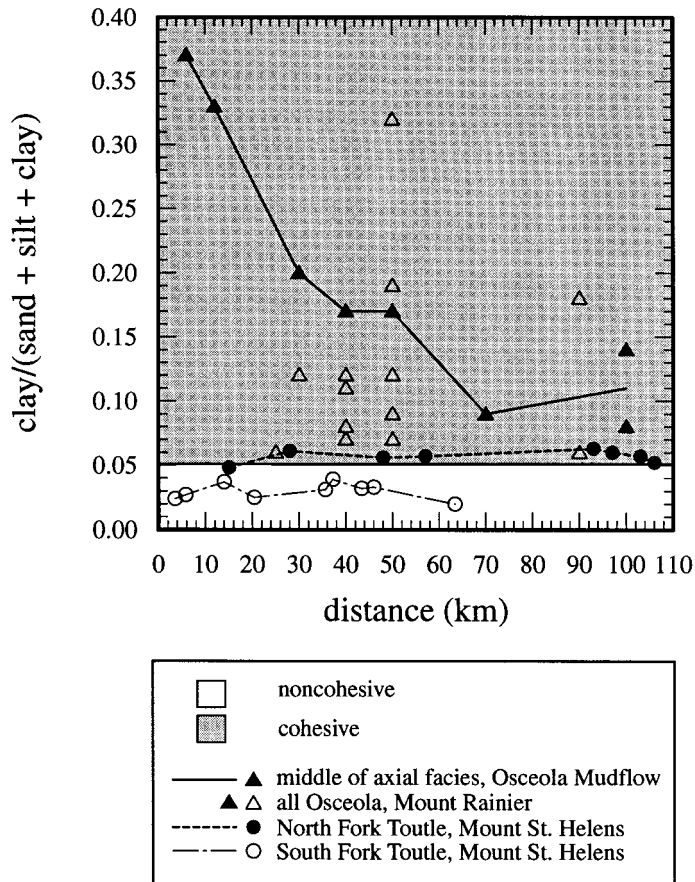


Figure 2. Graph showing  $clay/(sand + silt + clay)$  of cohesive and noncohesive lahars from Mount Rainier and Mount St. Helens versus downstream distance from the volcano.

stream to more dilute flows, and cohesive flows, which typically begin as water-saturated avalanches that transform downstream to debris flows and remain debris flows to their termini. Because the terms are defined by *clay* in the matrix rather than by their origin or their tendency to transform downstream to hyperconcentrated flow, some cohesive lahars like the North Fork lahar (Fig. 2) and the Paradise lahar (Scott et al., 1995) straddle the boundary. The term bulking is used as a general term for the incorporation of sediment in a flow by erosion at the flow boundary (Scott, 1988). In contrast to general deposition of bulk sediment, debulking is used as a term for the preferred deposition of certain particle sizes (generally coarse particles) from the flowing debris as it moves downstream.

## TOPOGRAPHIC AND GEOLOGIC SETTING

Mount Rainier volcano is the highest (4392 m) and most extensively glaciated peak in the Cascade Range. Glacier ice covers 92 km<sup>2</sup> of the volcano and has a volume of 4.4 km<sup>3</sup> (Driedger and Kennard, 1986). The Emmons glacier (11.2 km<sup>2</sup> area, 0.67 km<sup>3</sup> volume) and Winthrop Glacier (9.1 km<sup>2</sup> area, 0.52 km<sup>3</sup> volume) descend the northeast and north sides of Mount Rainier at the headwaters of the Main and West forks of the White River. These two rivers flow northeast and north from Mount Rainier, join about 45 km downstream near Greenwater, and flow westward to Puget Sound (Fig. 1).

The Puget Sound lowland in the vicinity of the Osceola Mudflow is underlain by glacial drift of Vashon age (Crandell, 1963b; Mullineaux, 1965a, 1965b). The last major (Vashon) advance of the Puget glacier lobe during

the Fraser glaciation banked up against the Cascade Range mountain front at the mouth of the White River during late Wisconsin time and formed a sequence of kame terraces that extends almost 10 km up the White River drainage near Mud Mountain (Fig. 1). The glacier retreated from the mountain front by about 12 000 yr B.P., leaving the White River flowing westerly across the Puget Sound lowland along the present course of South Prairie Creek (Fig. 1; Crandell, 1963b). Alpine glaciers of Evans Creek age covered much of Mount Rainier and vicinity, advanced to within several kilometres of the confluence of the West and Main forks of the White River, then retreated by about 17 000 yr B.P. (Crandell and Miller, 1974). Three exotic tephros and one from Mount Rainier are useful stratigraphic markers in the White River valley, because they are widespread and easily identified in the field. The tephros include layer O from Mount Mazama, layer Y from Mount St. Helens, layer C from Mount Rainier, and layer Wn from Mount St. Helens (Mullineaux, 1974) (Table 1).

## AGE, ORIGIN, AND STRATIGRAPHIC RELATIONSHIPS OF THE OSCEOLA MUDFLOW

### Age of the Osceola Mudflow

Eight radiocarbon ages on wood from Osceola Mudflow deposits range from 4425 ± 310 to 5040 ± 150 yr B.P. (Table 2, numbers 1, 3, 4, 6, 7, 9, 10, and 12). The 4425 ± 310 yr B.P. age on wood from a quarry near Huckleberry Creek (sample 1, Table 2) seems anomalously young, but a second age, 4980 ± 200 yr B.P. (sample 9, Table 2), on wood from the same outcrop, is within the range of anticipated statistical error for the samples. The average of the eight radiocarbon ages with one standard deviation of confidence is 4832 ± 43 yr B.P. (Stuiver and Reimer, 1993). The average age of the Osceola Mudflow, corrected for changes in atmospheric <sup>14</sup>C, is between 5603 and 5491 yr B.P. and has a calibration-curve intercept of 5588 yr B.P. (Stuiver and Reimer, 1993). The calendar age of the Mudflow is thus about 5600 yr B.P.

### Source of the Osceola Mudflow

Several authors (Russell, 1898; Matthes, 1914; Coombs, 1936; Fiske et al., 1963; Crandell, 1963a) recognized that Mount Rainier was once higher than it is now. Crandell (1963a) first inferred that the "missing summit" had avalanched down the northeast side of Mount Rainier to form the Osceola Mudflow. The resulting depression might have had the form of a semicircular amphitheater open to the northeast. The depression has since largely been filled by ice and by lava flows extruded at a central vent, but Russell Cliff, Liberty Cap, Point Success, and Disappointment Cleaver still define part of its outline (Figs. 1 and 3). The volume of the missing summit can be calculated by noting that the outline of the depression is about 1.8 km across and inferring the original height of the summit and depth of the depression. By projecting dipping lava beds upward, Fiske et al. (1963) estimated the pre-Osceola height of Mount Rainier as ≈4900 m. The outlines of the Mount St. Helens, May 18, 1980 crater (2 km across) and the Osceola depression (1.8 to 2.0 km across) suggest that they are similar in size. Therefore, we assume that the depth of the Osceola depression was about 0.6 km, about the depth of the Mount St. Helens crater. Assuming that the missing volume of Mount Rainier can be modeled as a cone and cylinder, each having a base of 1.8 to 2 km in diameter and a height of 0.6 km, the missing volume of Mount Rainier is calculated to be 2.0 to 2.5 km<sup>3</sup>.

An important discovery (Crandell, 1971) was the presence of clay and other alteration minerals like smectite, kaolinite, halloysite, mica, cristobalite, opal, and hematite in Osceola deposits. Frank (1985; 1995) later discovered the same minerals in outcrops of hydrothermally altered rock high on the edifice. The presence of these distinctive alteration minerals within

TABLE 1. AGES AND DISTINGUISHING CHARACTERISTICS OF IMPORTANT TEPHRAS AT MOUNT RAINIER

Tephra unit	Source volcano	Age (years B.P.)	Distribution	Thickness (cm)	Grain size (mm)	Other
W <sub>n</sub>	St. Helens	A.D.* 1480	Eastern half of study area	0–4	< 2	White sand-sized pumice near surface
C	Rainier	2200	East to north-northeast of summit	0–30	5–50	Brown pumice scoria and lithic lapilli at surface
Y	St. Helens	3500 <sup>†</sup>	Eastern two-thirds of study area	0–25	0.5–3	Yellow coarse sand-sized pumice and several fine-grained layers
B	Rainier	ca. 4500 to 4800	Southeast to east of summit	0–7	1–50	Reddish-brown ash with scattered bombs and lapilli
H	Rainier	ca. 4500 to ca. 4800	Southeast to east-northeast of summit	0–5	1–10	Brown to gray ash with scattered lapilli
F	Rainier	ca. 4800	South-southeast to north-northeast; lowest unit is to the northeast	0–15	0.002–10	Light colored clayey ash and scattered lapilli, three layers
S	Rainier	4800 to 5000	Northeast of summit, narrow lobe	0–150	0.5–1000	Angular blocks in gray ash
N	Rainier	4800 to 5200	East-southeast to northeast of summit	0–4	1–10	Reddish-brown lapilli in coarse ash
D	Rainier	5800 to 6400	East-southeast to east-northeast of summit	0–15	50–200	Reddish-brown scoria and lapilli
L	Rainier	6400	Southeast to east of summit	0–20	<50	Brown pumice between dark gray ash beds
A	Rainier	6400 to 6700	Southeast to north-northeast	0–3	<30	White pumice in brown ash
O	Mazama	6850 <sup>§</sup>	Eastern two-thirds of study area	2–4	0.01–0.4	Orange to cream colored very fine sand- to silt-sized ash

*Note:* Adapted from Mullineaux (1974). Unless otherwise noted, ages are given in terms of radiocarbon years B.P.  
\*Yamaguchi (1983)—a calendar age based on correlation of tree rings.  
<sup>†</sup>Mullineaux (1986).  
<sup>§</sup>Bacon (1983).

remnants of the pre-Osceola edifice and within Osceola deposits indicates that the Mudflow began as a huge avalanche of previously altered rock (Crandell, 1971).

#### Relation of the Osceola Mudflow to Tephra Layers F and S

Tephra layer S (Table 1) comprises a poorly sorted mixture of angular fragments and ash of lithic Mount Rainier andesite, which crops out along the ridge between Dege Peak and Sunrise in Mount Rainier National Park (Mullineaux, 1974). The tephra overlies tephra layers O and D (6850 yr B.P. and 5800 to 6400 yr B.P., Table 1) and directly underlies tephra layer F. On Goat Island Mountain, a runup deposit of the Osceola Mudflow overlies, with no intervening weathering zone, 2 or more meters of Mount Rainier andesite rubble that we interpret as layer S. Crandell (1971) suggested that layer S might be associated with the eruption that produced the Greenwater lahar; we agree with Crandell, but believe that the Greenwater is really part of the Osceola Mudflow.

Mullineaux (1974) inferred that the Osceola Mudflow and tephra layer F were genetically related because he observed similar clay minerals like smectite, kaolinite, and mixed layer clay in both of these units but not in other lahars and tephra layers of similar age. A radiocarbon date from peat beneath set F coincides with older limiting dates for the Osceola Mudflow (Table 2). We discovered a remnant of layer F overlying an Osceola deposit

that was emplaced when the Mudflow ran more than 100 m up on the flank of Goat Island Mountain (along a ridge to the north at an altitude of 2054 m). Otherwise, tephra set F is not present on top of the Osceola Mudflow despite the presence of that layer on valley sides and ridge tops adjacent to deposits of the Osceola (Mullineaux, 1974; this study). Further, the Osceola Mudflow rests directly on Pleistocene till, bedrock, or noncohesive lahar deposits rather than set F within the tephra's known area of extent. These relationships are consistent with the fall of tephra set F after initiation of the Osceola Mudflow but, at most localities, before it stopped moving. Its position high on a ridge crest directly opposite Mount Rainier suggests that the runup debris was part of the leading edge of the Osceola avalanche, and we infer that the runup was deposited early in the eruption sequence, before or during the fall of tephra set F.

Mullineaux found that set F consists of at least three layers. The oldest layer, F<sub>1</sub>, is mainly distributed northeast of the volcano and is composed primarily of lithic fragments and clay minerals; the second layer, F<sub>m</sub>, is distributed east to southeast of Mount Rainier, contains some lithic ash, but is mainly composed of pumice and pyrogenic crystals; the third layer, F<sub>u</sub>, is also distributed to the northeast and includes abundant clay minerals and lithic fragments as well as significant proportions of pumice and broken pyrogenic crystals (Fig. 1). The three layers are inferred to have been deposited within a short time, perhaps less than an hour, because no evidence of erosion or weathering exists between them.

TABLE 2. RADIOCARBON AGES PERTAINING TO THE OSCEOLA MUDFLOW

Sample number	Radiocarbon age	Unit and stratigraphic position	Sample description and locality
1	4425 ± 310	Osceola Mudflow	Bark from an outcrop at a quarry near Huckleberry Creek
2	4625 ± 240	Paradise lahar	Charcoal from an outcrop near Ricksecker Point
3	4700 ± 250	Osceola Mudflow	Wood from an outcrop along the bank of the Puyallup River near Sumner
4	4700 ± 60	Osceola Mudflow	Wood from an outcrop along the bank of the Puyallup River near Sumner
5	4730 ± 320	Paradise lahar	Charcoal fragments from near the upper part of the deposit, Nisqually River valley near National
6	4800 ± 300	Osceola Mudflow	Log from an outcrop near Mud Mountain Dam
7	4950 ± 300	Osceola Mudflow	Log from an outcrop along a roadcut of Highway 410 near Buckley
8	4955 ± 585	Soil layer underlying the Paradise lahar and overlying layer O	Wood from an outcrop near Longmire
9	4980 ± 200	Osceola Mudflow	Wood from an outcrop at a quarry near Huckleberry Creek
10	5010 ± 80	Osceola Mudflow	Twigs from a well boring 4 km north of Sumner
11	5020 ± 300	Soil horizon below tephra layer F	Peat from below tephra layer F in Cowlitz Park 6 km southeast of Mount Rainier
12	5040 ± 150	Osceola Mudflow	Wood from a depth of 80 m in a well boring near Auburn
13	5230 ± 235	Soil horizon below the Osceola Mudflow and 2 older lahars but above layer O	Charcoal fragments in an organic-rich soil zone exposed along the White River about 1 km upstream of Buck Creek
14	6075 ± 320	Lahar underlying two pre-Osceola lahars	Wood fragment from a lahar exposed along the White River about 1 km upstream of Buck Creek

Note: Samples 1, 2, 5, 8, 9, 13, and 14 are from Scott et al. (1992); samples 3, 6, and 7 are from Crandell (1963b); sample 11 is from Mullineaux (1974); samples 4 and 10 are from Dragovich et al. (1994); and sample 12 is from Luzier (1969). More complete locality descriptions were given in those papers.

Tephra layers S,  $F_1$ , and  $F_u$  all have characteristics that suggest laterally directed, phreatic or phreatomagmatic eruptions. The distribution of these layers in narrow lobes suggests explosions with strong lateral components or vertical eruption during very strong unidirectional wind. Each of the lobes has an axis that roughly corresponds to the medial axis of the scarp inferred to have been left by the Osceola sector collapse (Fig. 1). Such a coincidentally fortuitous wind direction seems unlikely, especially because the dominantly magmatic tephra layer,  $F_m$ , is distributed in a broad arc east-southeast of the volcano rather than northeast like the others (Fig. 1). Tephra layer S is limited to a very narrow lobe to the northeast and contains angular blocks that can have no origin other than as laterally projected ballistic fragments (Mullineaux, 1974). The deposit contains no juvenile material and thus probably resulted from phreatic explosions. Tephra layer  $F_1$  comprises lithic lapilli, hydrothermal clay minerals, and minor amounts of juvenile pumice, glass shards, and crystals that suggest the addition of a

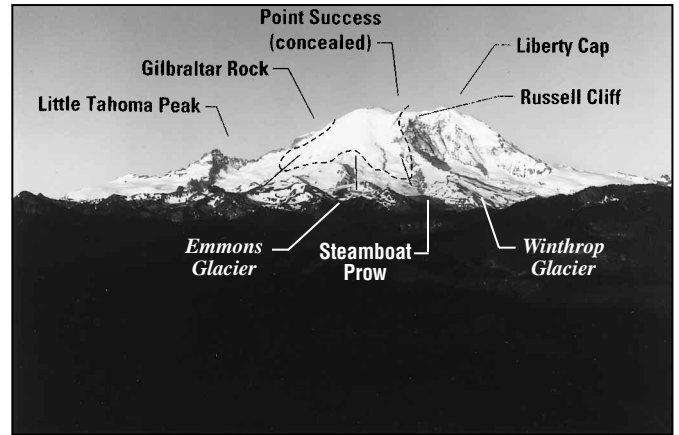


Figure 3. Photograph of Mount Rainier from north, showing post-Osceola edifice filling Osceola avalanche scarp, defined by Disappointment Cleaver, Russell Cliff, Liberty Cap, and Point Success (not in the field of view).

magmatic component. After the magmatic eruption of  $F_m$ , tephra layer  $F_u$ , with its increased proportion of hydrothermal clay, its substantial proportion of juvenile particles, and its distribution to the northeast, indicates a return to phreatomagmatic explosions.

The Osceola Mudflow is about an order of magnitude larger than the other cohesive lahars that occurred at Mount Rainier during Holocene time and is the only one clearly related to an eruption. The intrusion of magma to shallow depths and explosive activity during the eruption of tephra layer F probably contributed to the destabilization of a large volume of the edifice and to the enormous size of the Mudflow.

#### Relation of the Osceola Mudflow and the Paradise Lahar

The Paradise lahar is a large ( $50$  to  $100 \times 10^6$  m<sup>3</sup>; Crandell, 1971) cohesive lahar that crops out in the Nisqually River valley at least as far downstream as National (Fig. 1). The lahar originated in avalanches of partly altered rock near the summit. It temporarily filled valleys to depths as great as 300 m but attenuated rapidly downstream (Crandell, 1971). Its downstream equivalent is not observed below National, but it probably extended farther (Scott et al., 1995). Despite the tremendous depths to which it filled valleys, the lahar left behind only thin (0.5 to 2 m thick) deposits and failed to erode the even thinner (less than 5 cm) deposits of layer O at many locations on valley-side slopes. Its voluminous, sharply peaked, and rapidly attenuating character records the sudden collapse of a portion of the upper cone, possibly triggered by explosions associated with layer S or  $F_1$ . Both the smaller clay-size fraction and clay-mineral content of the deposits relative to those of the Osceola Mudflow deposits suggest an origin from less-altered parts of the edifice.

Stratigraphy and radiocarbon ages suggest that the Osceola Mudflow and the Paradise lahar are coeval (Scott et al., 1995). On the valley side about 300 m above the headwaters of the Nisqually River, scattered lapilli of layer  $F_m$  overlie the Paradise lahar. Charcoal fragments from within the lahar at two localities have ages of  $4625 \pm 240$  and  $4730 \pm 320$  yr B.P., and a third age on wood from a soil beneath the lahar is  $4955 \pm 585$  yr B.P. (Table 2). The average of the first two radiocarbon ages,  $4663 \pm 192$  (Stuiver and Reimer, 1993), overlaps and is thus consistent with the radiocarbon age of the Osceola Mudflow. The average age of the Paradise lahar, corrected for changes in atmospheric <sup>14</sup>C, is between 5596 yr B.P. and 5048 yr B.P. and has calibration-curve intercepts of 5443, 5414, and 5324 yr B.P. (Stuiver and Reimer, 1993).

**Eruption Narrative**

Sometime after about 5200 <sup>14</sup>C yr B.P. but before the Osceola Mudflow was formed, pyroclastic eruptions produced pumice and ash of tephra layer N that were deposited east and northeast of the volcano (Fig. 4). At least three noncohesive lahars flowed down the White River drainage at about this same time, and one or more moved as far as the Puget Sound lowland (Buck Creek lahar assemblage, Fig. 4). Two of the lahars contain breadcrusted bombs near the volcano, and all contain fresh angular blocks of andesite from Mount Rainier; these observations suggest that the lahars formed when hot pyroclastic debris avalanched down the Emmons and Winthrop Glaciers. The presence of breadcrusted bombs in the lahars suggests that they were formed during pyroclastic eruptions by pyroclastic flows or hot avalanches that swept across firm and glacier ice. Whether the same eruption produced layer N and the lahars is not known, but the similar time constraints (Fig. 4) suggest that the eruptions could be genetically related.

There was a repose of as much as several hundred years or as little as a few hours, then the eruptive sequence that triggered the Osceola Mudflow, recorded by tephra layers S(?), F<sub>1</sub>, and F<sub>m</sub>, apparently began with phreatic explosions, progressed through phreatomagmatic explosions to magmatic activity, and finally retrogressed to mixed phreatic explosions and magmatic activity. The sequence of tephras with apparent lateral components, S, F<sub>1</sub>, and F<sub>v</sub>, shows an increase in content of hydrothermal clay minerals with time and suggests that as the eruption progressed it involved rocks deeper within the edifice.

Edifice construction ensued for several centuries after the climactic Osceola event. The eruption of small volumes of tephra (layers H and B) probably corresponds to minor explosive activity that occurred during this period of magmatism. The tephra stratigraphy suggests that explosive activity at Mount Rainier ceased for nearly 2000 yr after ca. 4500 yr B.P. By the time Mount Rainier became active again, ca. 2300 yr B.P., the depression had been filled by nonexplosive lava flows so that pyroclastic flows from the central vent spilled westward into the Puyallup River drainage.

**DISTRIBUTION, VOLUME, AND PHYSICAL CHARACTERISTICS OF THE OSCEOLA MUDFLOW**

The distribution of the Osceola Mudflow is shown in Figure 1. Within about 8 km of its source, the proximal part of the deposit is present on Steamboat Prow, in the Inter Fork valley, and on ridges overlooking the Winthrop Glacier. Below the Winthrop and Emmons Glaciers and down valley for about 70 km, the medial part is present throughout the Main and West Forks of the White River valley. Typically the Osceola Mudflow forms 5–20-m-thick fills in valley bottoms and 30–200-cm-thick veneers on steep valley sides as much as 200 m above the present river level. Its distal part blankets 211 km<sup>2</sup> of the Puget Sound lowland (Crandell, 1971) and underlies ≈157 km<sup>2</sup> of the now-sediment-filled Duwamish and Puyallup embayments of Puget Sound, where water wells penetrate the deposit at depths of up to 100 m (Dragovich et al., 1994).

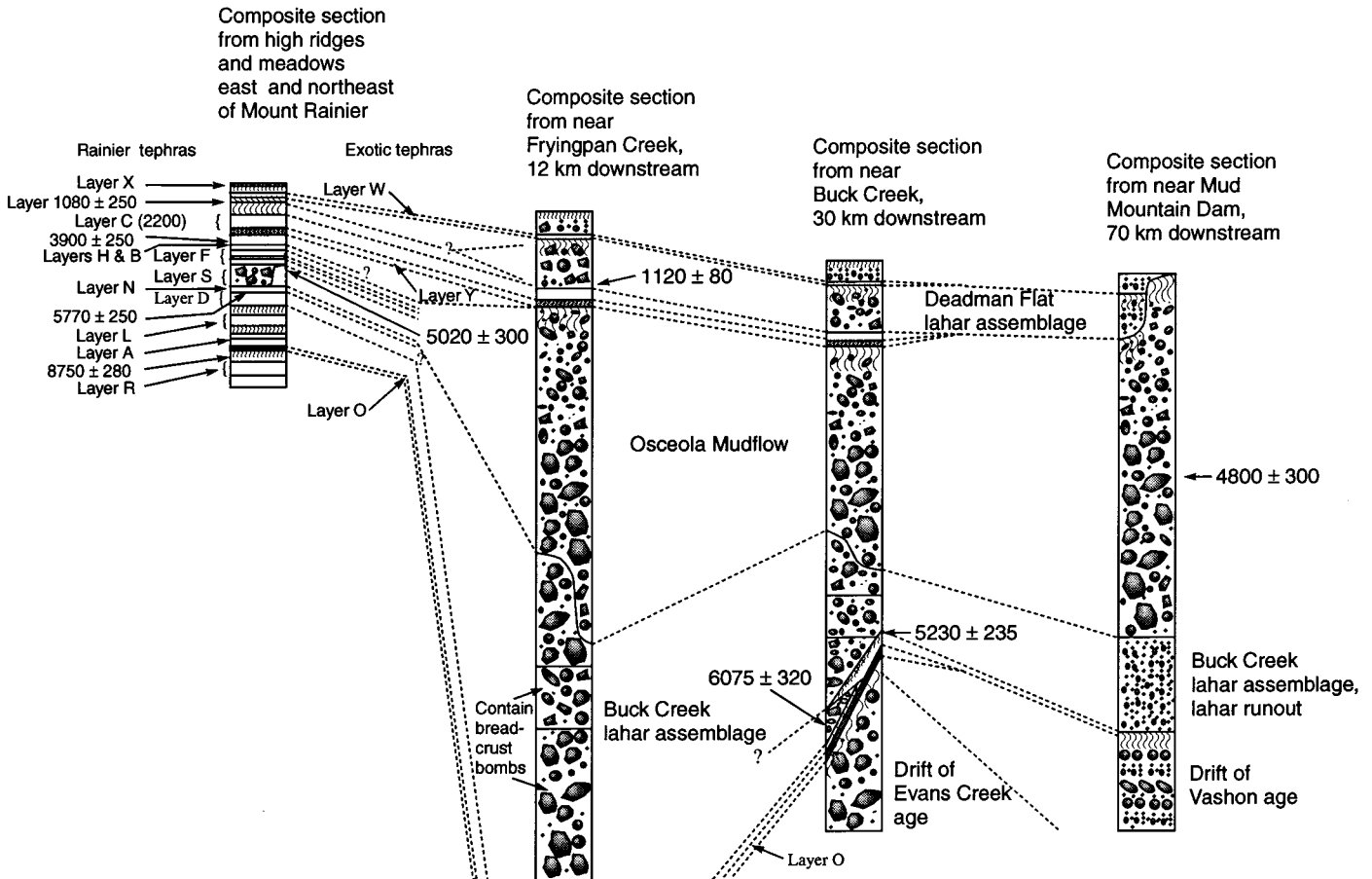


**Figure 4. Schematic sections showing relationship between tephra layers and lahar assemblages in White River drainage basin.**

TABLE 3. ORIGINAL AREA AND VOLUME OF THE OSCEOLA MUDFLOW

Location	Area (km <sup>2</sup> )	Volume (× 10 <sup>6</sup> m <sup>3</sup> )
Valleys upstream from Puget Sound lowland	150	930
Puget Sound lowland	212	1370
South Prairie Creek and Puyallup River valleys (all subsurface)	28*	240*
Puyallup and Duwamish embayments of Puget Sound 5600 yr B.P. (all subsurface)	157*	1260*
Total	547 <sup>†</sup>	3800 <sup>†</sup>

\*Subsurface data from Dragovich et al. (1994).  
<sup>†</sup>Total area and volume are minimum values.

### Volume of the Osceola Mudflow

The volume of 3.8 km<sup>3</sup> given for the Osceola Mudflow in Table 3 is based on examination of outcrops, analysis of more than 200 well logs, and data provided to us by Joe Dragovich and Pat Pringle of the Washington Department of Natural Resources. To compute the volume, the areal extent of the deposit was divided into 25 parcels and an average thickness was determined for each parcel. The volumes of the parcels were then summed and averaged over distance to find the center of mass. The center of mass of the Osceola deposit is located about 80 km downstream from Mount Rainier. The Osceola volume of 3.8 km<sup>3</sup> plus the Paradise volume of 0.05 to 0.1 km<sup>3</sup> is more than the 2 to 2.5 km<sup>3</sup> volume of the "missing summit." Dilation of the original avalanche mass and bulking of exotic material account for the difference in volume.

Appreciable volumes of Osceola debris underlie the Puyallup River valley and the Puyallup and Duwamish embayments of Puget Sound (Fig. 1). Luzier (1969) discovered the Osceola Mudflow at a depth of about 80 m (about 60 m below sea level) in a well 5 km north of Auburn and obtained a radiocarbon age of 5040 ± 150 (Table 2, no. 10) on wood from the 10-m-thick deposit. Wells near Orting in the Puyallup valley penetrate thicknesses of 6 to 8 m at a depth of about 6 m; down valley, near Sumner on the subtidal to tidal Auburn and Puyallup deltas, the Mudflow forms fills 20 to 30 m thick (Dragovich et al., 1994). From their inspection of more than

700 well logs, Dragovich and his colleagues concluded that at least 1.26 km<sup>3</sup> of Osceola debris spread underwater and covered at least 157 km<sup>2</sup> in Puget Sound. The tremendous volume of Osceola debris and greatly increased sedimentation during post-Osceola time combined to fill the Duwamish and Puyallup arms of Puget Sound.

### Axial, Valley-Side, and Hummocky Facies

In his study of the lahars of the Toutle River, Scott (1988) suggested that certain units are distinctive enough to be recognizable as facies and that each facies represents a different environment within the flow. The facies recognized in the huge, locally hummocky, and cohesive Osceola Mudflow are broadly similar to those recognized in smaller cohesive and noncohesive lahars, but they differ significantly because of the differing origin and behavior of the Osceola. The three facies defined here are (1) the axial facies, including deposits thicker than about 2 m on terraces along mountain valleys and deposits in the Puget Sound lowland, (2) the valley-side facies, where debris deposited on steep slopes at high stages later drained into valley bottoms, and (3) the hummocky facies, characterized by numerous mounds and hummocks formed mostly of huge, relatively intact fragments of the original edifice.

**Axial Facies.** The Osceola Mudflow filled the mountain valleys to such great depths that the entire flood plain and terraces up to about 30 m higher may be regarded as the channel. The axial-fill deposits in this reach form flat surfaces or surfaces that gently slope toward river channels. The Mudflow's surface in the Puget Sound lowland is flat. Thick, axial deposits are massive, poorly sorted mixtures that exhibit a striking decrease in the number of gravel-sized particles from bottom to top (Fig. 5). In the lowland, deposits thin toward topographic highs and toward distal margins (Crandell, 1963b). Lowland deposits less than about 1.5 m thick are not obviously graded and resemble the upper part of nearby thicker deposits.

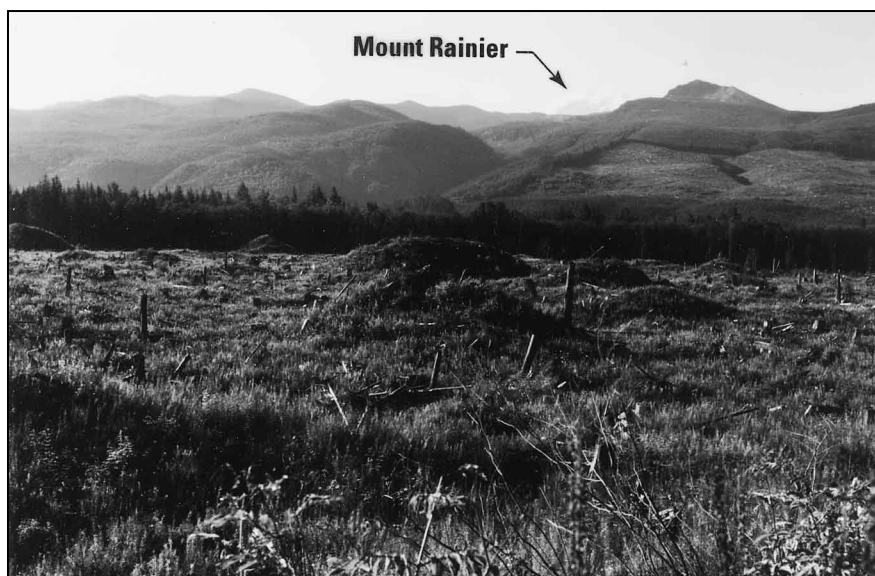
Deposits thicker than about 3 m have pinkish-gray bases with abundant wood fragments and yellowish-gray tops with abundant wood casts but no wood. Wood is apparently destroyed by bacteria in the aerated upper zone (Vallance, 1994a). The two zones are separated by one or several bands of iron-stained cement that form at the fluctuating water table. A similar rust-colored, indurated hardpan commonly exists in underlying deposits at their contact with the Osceola Mudflow. Air trapped in the pore space of the underlying deposit apparently reacted with aqueous iron and silica that migrated down from the mudflow, and precipitated as oxides to form the



Figure 5. Photograph showing 8-m-thick, normally graded outcrop of Osceola Mudflow near town of Greenwater. Large boulders in the foreground are ≈2 m in maximum dimension.

Osceola Mudflow

Lahar runout of Buck Creek assemblage



**Figure 6.** Photograph showing hummocks on the surface of the Osceola Mudflow about 1 km east of Scatter Creek and about 70 km downstream from Mount Rainier. Hummocks in the foreground are 15 to 40 m in diameter. Mount Rainier is in the background.

hardpan. The hardpan did not form in underlying materials that were water saturated when the Osceola was deposited.

**Valley-Side Facies.** The valley-side facies represents peak inundation at diminishing stage heights that are modified by local conditions and by subsequent down-slope drainage during waning flow. The surfaces of valley-side deposits of the Osceola Mudflow conform closely to the previous underlying topography. Because of subsequent weathering and slope processes, most of these valley-side deposits are now recognizable only by the presence of rounded pebbles and cobbles and exotic lithologies in the soil overlying tephra layer O or colluvium. Where they have not been destroyed by weathering, valley-side deposits are unsorted and ungraded mixtures of pebbles, cobbles, and boulders in a clay, silt, and sand matrix.

**Hummocky Facies.** At seven places in the White River valley between Mount Rainier and Mud Mountain Dam, hummocks as high as 20 m and as wide as 60 m dot the surface of the deposit (Fig. 6) and define the hummocky facies. Groups of hummocks are especially common on high terraces and in tributary valleys, several of which were regarded by Crandell (1971) as deposits of the Greenwater lahar. Water wells encountered andesite megablocks at depths of 10 to 20 m in the Greenwater area. Although the megablock-rich zone is not exposed in the valley bottom, well logs suggest that the megablocks are in a cohesive matrix under 5 to 15 m of more clay-rich Osceola debris. This megablock-rich zone suggests the presence of the hummocky facies at depth in the Greenwater area.

#### **Relationship Between the Osceola Mudflow and the Greenwater Lahar**

Crandell (1971) described the Greenwater lahar as a hummocky, clay-poor lahar that filled the valley of the Main Fork of the White River to a depth greater than that of the subsequent Osceola Mudflow. Crandell's (1971, Fig. 6) mapping confines the Greenwater deposits to fills in tributary valleys, 30 to 100 m above the present river level, at four localities. He distinguished the Greenwater lahar from the Osceola Mudflow by its higher topographic position, its topographic expression (presence of hummocks), and its lack of clay-rich matrix, but did not observe an overlapping relation between the two deposits.

Evidence uncovered at new exposures, new clear cuts, and backhoe trenches at two of Crandell's localities suggest the simpler explanation that the Greenwater lahar is a hummock-rich facies of the Osceola Mudflow.

Near Huckleberry Creek, a gravel quarry exposes 5 m of typical (i.e., yellowish- to pinkish-gray top to bottom, clay-rich, and normally graded) axial facies Osceola Mudflow above 6 m of Evans Creek outwash gravel. The quarry is on a terrace within 180 m of hummocky terrain on the same terrace, mapped by Crandell (1971) as Greenwater lahar (Fig. 1). Joe Ensley and Neil Crawford of White River National Forest assisted in digging two backhoe trenches next to the nearest hummocks and two more between the hummocks and the gravel quarry. The 4-m-deep trenches revealed only one lahar deposit underlying the terrace in this area. Furthermore, the blocks that form the hummocks are "floating" in a clay-rich matrix similar to that at the quarry (Table 4).

Stratigraphic relations and inundation-limit mapping near Buck Creek are incompatible with defining the Greenwater lahar as a distinct unit. A backhoe trench at Crandell's Greenwater locality near Buck Creek revealed, from the top down, tephra layer Wn, a noncohesive debris flow, tephra layers C and Y, and a hummock-forming block of Mount Rainier provenance surrounded by clay-rich matrix like that of the axial facies of the Osceola Mudflow. About 300 m downslope from this site a similar sequence is observed. There the sequence is tephra layer Wn, a noncohesive debris flow, tephra layers C and Y, the 6–8-m-thick, normally graded axial facies of the Osceola Mudflow, three noncohesive debris flows, a soil, tephra layer O, a soil, and glacial drift of Evans Creek age (Fig. 4). Crandell's interpretation of the Greenwater lahar as an older larger flow implies that the Osceola Mudflow has an inundation limit of 780 m (Fig. 7A, section 1). On the basis of a well log 4 km upstream, Crandell (1971) suggested that degradation had deepened the valley in pre-Osceola time, but the sequence underlying the Osceola Mudflow (the Buck Creek lahar assemblage, a soil, tephra layer O, a soil, and Evans Creek drift; Fig. 4) indicates aggradation of the valley instead. Crandell's (1971) interpretation thus requires an improbably small Osceola cross section in comparison to those upstream and downstream (Fig. 7A).

#### **Origin of Water in the Osceola Mudflow**

Water in the debris flow includes that derived from the preexisting rocks of the volcano and that admixed with the debris during transport. Because the Osceola Mudflow has a volume of at least 3.8 km<sup>3</sup>, a large volume of water was required to saturate it. Samples of Osceola deposits with clay contents that range from 6% to 12% and average 8% have liquid limits that

OSCEOLA MUDFLOW, MOUNT RAINIER

TABLE 4. GRAIN-SIZE ANALYSES OF THE OSCEOLA MUDFLOW

Sample	Unit, facies	Distance downstream (km)	Position	Size fractions (%)				Ratio sand:silt:clay	Mean*		Sorting*		Skewness*		Kurtosis* $K_G$
				gravel	sand	silt	clay		$M_d$	$M_z$	$\sigma_G$	$\sigma_I$	$Sk_G$	$Sk_I$	
1.	Proximal, axial	5	50 m above valley, middle of 60 m thick deposit	60.1	14.2	10.9	14.8	36:27:37	-1.7	-0.1	6.1	7.9	+0.41	+0.53	1.55
2.	Proximal, axial	12	25 m above valley bottom	53.9	21.1	9.7	15.3	46:21:33	-1.8	-0.3	6.0	7.0	+0.38	+0.47	1.28
3.	Medial, valley-side	25	110 m above valley bottom (West Fork)	66.8	25.2	5.9	2.1	76:18:6	-4.3	-3.5	5.2	4.8	+0.22	+0.28	0.79
4.	Medial, axial	30	10 m above valley bottom	52.3	29.1	9.2	9.4	61:19:20	-1.4	-1.4	6.2	6.4	+0.01	+0.16	1.13
5.	Medial, hummocky <sup>†</sup>	30	50 m above valley bottom	56.6	28.9	9.3	5.2	67:21:12	-2.6	-3.1	5.1	5.0	+0.24	+0.29	0.91
6.	Medial, axial	40	20 m above valley bottom	63.6	22.9	7.4	6.1	63:20:17	-4.0	-2.9	5.8	5.7	+0.29	+0.38	0.87
7.	Medial, axial to hummocky <sup>†</sup>	40	22 m above valley bottom	61.2	25.0	8.6	4.4	67:22:11	-3.8	-2.6	5.2	4.9	+0.35	+0.38	0.80
8.	Medial, axial to hummocky <sup>†</sup>	40	24 m above valley bottom	65.4	24.0	8.1	2.5	70:23:7	-4.6	-3.0	5.0	4.7	+0.49	+0.49	0.75
9.	Medial, hummocky <sup>†</sup>	40	25 m above valley bottom	40.9	41.9	12.3	4.4	70:22:8	+0.2	-0.03	4.5	4.3	-0.08	-0.003	0.84
10.	Medial, hummocky <sup>†</sup>	40	25 m above valley bottom	56.9	30.0	9.2	3.9	69:21:10	-2.8	-2.1	4.8	4.6	+0.23	+0.28	0.76
11.	Medial, valley-side <sup>§</sup>	40	Tributary valley 85 m above valley bottom	52.5	33.7	10.7	3.1	71:22:7	-1.8	-1.7	5.1	4.7	+0.04	+0.10	0.74
12.	Cohesive unit <sup>#</sup>	50	Deposit underlying Osceola in river bank	50.0	33.9	10.1	6.0	68:20:12	-1.0	-0.9	4.9	4.9	+0.02	+0.12	0.94
13.	Medial, axial	50	Base of 8 m thick deposit in river bank	78.0	16.2	4.2	1.6	74:19:7	-7.2	-5.7	4.6	4.5	+0.48	+0.54	0.95
14.	Medial, axial	50	Middle of 8 m thick deposit in river bank	59.5	26.5	7.2	6.8	65:18:17	-3.3	-2.7	5.9	5.9	+0.15	+0.27	0.85
15.	Medial, axial	50	Top of 8 m thick deposit in river bank	49.4	28.7	12.4	9.5	56:25:19	-0.9	-0.4	5.5	5.7	+0.15	+0.23	1.06
16.	Medial, valley-side	50	55 m above valley bottom	56.9	22.9	6.6	13.6	53:15:32	-3.0	-1.4	7.1	7.1	+0.34	+0.43	1.03
17.	Medial, valley-side	50	80 m above valley bottom	58.5	27.4	10.4	3.7	66:25:9	-3.1	-2.2	5.4	5.1	+0.24	+0.28	0.77
18.	Medial, axial	70	Kame terrace 90 m above present valley bottom	50.6	36.2	9.0	4.2	73:18:9	-1.2	-1.4	5.0	4.8	-0.05	+0.06	0.82
19.	Medial, axial	90	Puget Sound drift plain, base of deposit	59.4	29.3	9.0	2.3	72:22:6	-3.6	-2.6	5.1	4.8	+0.29	+0.30	0.76
20.	Medial, axial	90	Puget Sound drift plain top of deposit	47.1	29.5	13.7	9.7	56:26:18	-0.6	-0.3	5.9	5.7	+0.07	+0.15	0.89
21.	Medial, axial	100	Puget Sound	49.8	32.0	10.9	7.3	64:22:14	-1.0	-0.6	5.1	4.9	+0.11	+0.20	0.86

Note: Samples 5 and 7 to 10 are taken from the basal meter of 4-m-deep pits. All remaining samples are from natural outcrops in which there is continuous exposure of the mudflow to its base. Except where indicated, the sample is collected from the middle of the deposit. Proportions of gravel-sized particles larger than 16 mm were estimated by point counting at the outcrop using the method of Wolman (1954) as described in Scott (1988). Proportions of particles smaller than 16 mm and larger than 0.063 mm were analysed by wet sieving, and proportions of particles smaller than 0.063 mm and larger than 0.003 mm were determined by pipette analysis. Proportions of particles smaller than 0.003 mm were estimated by graphic extrapolation.

\*Folk (1980) gave the graphical statistics of grain-size distributions with cumulative frequency plotted as percentage of grains finer than each size class as  $M_d = \phi_{50}$ ;  $M_z = (\phi_{16} + \phi_{50} + \phi_{84})/3$ ;  $\sigma_G = (\phi_{16} - \phi_{84})/2$ ;  $\sigma_I = (\phi_{16} - \phi_{84})/4 + (\phi_5 - \phi_{95})/6.6$ ;  $Sk_G = (\phi_{16} + \phi_{84} - 2\phi_{50})/(\phi_{16} - \phi_{84})$ ;  $Sk_I = (\phi_{16} + \phi_{84} - 2\phi_{50})/2(\phi_{16} - \phi_{84}) + (\phi_5 + \phi_{95} - 2\phi_{50})/2(\phi_5 - \phi_{95})$ ; and  $K_G = (\phi_{95} - \phi_5)/2.44(\phi_{75} - \phi_{25})$ .

<sup>†</sup>Sampled from an area previously mapped by Crandell (1971) as Greenwater lahar. Samples 5, 9, and 10 were taken from backhoe pits adjacent to hummocks.

<sup>§</sup>Sampled from an outcrop near the inundation limit of the Osceola Mudflow in an area previously mapped by Crandell (1971) as Greenwater lahar. The deposit overlies tephra layer O.

<sup>#</sup>We infer that this unit is the hummocky facies of the Osceola mudflow, but no hummocks are present in the outcrop, and it could be an older deposit.

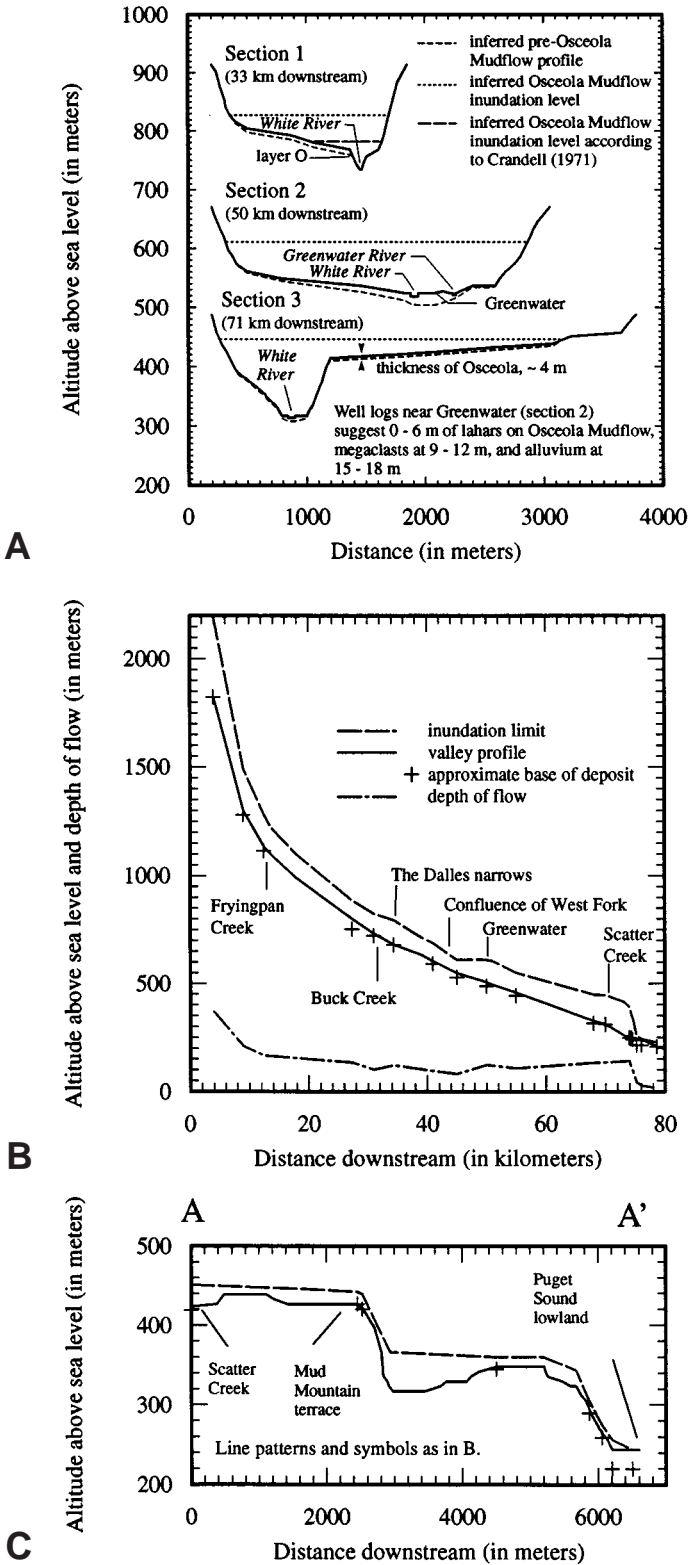


Figure 7. Cross-sections and longitudinal profiles showing White River valley and Osceola Mudflow at peak discharge. (A) Cross sections, viewed downstream, show maximum inundation limit of Osceola Mudflow at three sites. Locations of sections are shown in Figure 1. Vertical exaggeration, 5 $\times$ . (B) Profile along valley bottom of White River. (C) Profile A-A' near Mud Mountain dam. Location of section A-A' shown in Figure 1.

vary from 28% to 42% and average 33% (Crandell, 1971). An average water content of 33% for the Osceola implies that at least 1.27 km<sup>3</sup> of water would have been needed to liquify it, too much to be provided by rivers (containing only about 1% of the total needed).

The only possible sources for most of the water are glacial ice and snow, a crater lake, or pore water. Ice cannot readily be melted by cold sediment through frictional heating. For example, if 10% of the potential energy of the preavalanche mass were converted to heat that was efficiently transferred to the ice during subsequent flow, then frictional melting of ice and snow would contribute less than 3% of the water needed to fluidize the avalanching debris. Furthermore, there is no evidence of hot rock within the Osceola Mudflow. The water could have come from a crater lake, but, because the water was thoroughly mixed with the debris within 2 km of the source, it is more likely that widely dispersed hydrothermal or pore water was the primary source of the liquid. Clay in the hydrothermal system would have served to increase porosity, but more important, would have greatly reduced permeability. Thus, the large volume of hydrothermally altered, clay-rich rock that must have been present in the ancestral edifice of Mount Rainier probably stored a large volume of water in its pore space.

**BEHAVIOR OF THE OSCEOLA MUDFLOW**

Near Mount Rainier, deposits of the Osceola Mudflow cap ridges high above the Winthrop and Emmons glaciers. Remnants also occur on top of Steamboat Prow and throughout the Inter Fork drainage basin. The homogeneity of these deposits, the lack of hummocky terrain within 10 km of the summit, and the apparent fluidity suggest that the avalanches that initiated the Osceola Mudflow mixed thoroughly within 2 km of their source and abruptly began to behave like an enormous water-saturated debris flow.

Inundation-limit mapping along the steep-sided White River valley between Mount Rainier and Mud Mountain, 75 km downstream, reveals that the peak-stage height of the Osceola Mudflow attenuated sharply near the volcano, then reached an equilibrium downstream (Fig. 7B). In the Inter Fork valley, deposits of the mudflow are present 400 m above the valley bottom. The inundation limit is 200 m 5 km downstream; farther downstream, it stabilizes, varies between 85 m and 140 m, and averages about 100 m. The decrease of the maximum inundation depth downstream by longitudinal spreading and by deposition was counteracted by the additional discharge from the West Fork 45 km downstream and by bulking of the flow through the incorporation of eroded sediment.

Mud and debris of the Osceola Mudflow that ran up onto Goat Island Mountain, about 10 km from Mount Rainier, and onto a ridge dividing the White and Greenwater rivers, about 45 km downstream of Mount Rainier, allow the maximum velocity and peak discharge of the flow to be estimated at these two places (Fig. 1). Clay-rich Osceola debris is present to an altitude of 2127 m on Goat Island Mountain, but not just up valley at an altitude of 1944 m at the top of a low divide between Emmons Glacier and Fryingpan Creek. The debris on Goat Island Mountain suggests that the Osceola Mudflow ran up 180 m. Using  $v = (2gh)^{1/2}$ , where  $v$ ,  $g$ , and  $h$  are velocity, gravitational acceleration, and run-up height, the velocity of the flow must have been at least 60 m/s. Taking a typical nearby cross-sectional area in the Main Fork valley of about 190 000 m<sup>2</sup> suggests a discharge of  $\approx 11.4 \times 10^6$  m<sup>3</sup>/s. If the velocity was the same about 10 km downstream in the West Fork valley, a typical cross-sectional area of about 80 000 m<sup>2</sup> suggests a discharge of  $\approx 4.8 \times 10^6$  m<sup>3</sup>/s there and a simultaneous discharge of about  $16.2 \times 10^6$  m<sup>3</sup>. Similarly, at the confluence of the West and Main forks of the White River, mud and debris of the West Fork flow that ran up about 18 m onto a ridge dividing the White and Greenwater rivers (Fig. 1) allow a maximum velocity of 19 m/s to be estimated. Taking a typical nearby cross-sectional area in the West Fork valley of at least 70 000 m<sup>2</sup> suggests a discharge of  $\approx 1.3 \times 10^6$  m<sup>3</sup>/s. If the simultaneous dis-

charge along the Main Fork was as large, then the total discharge of the Osceola Mudflow near the confluence of the two forks of the White River would have been about  $2.6 \times 10^6 \text{ m}^3/\text{s}$ .

The tremendous discharge of the Osceola Mudflow from both forks of the White River and a constriction in the valley about 3 km downstream from the town of Greenwater caused hydraulic damming to an altitude of 609 m in the Greenwater area (Fig. 7, A, section 2; and B). The valley is 2 to 3 km wide in this area, so peak inundation was only about 100 m. Upstream, Osceola deposits also occur at an altitude of 609 m in the Greenwater River drainage, north of the ridge that divides the Greenwater and White rivers. Those deposits suggest that the lahar backed up the Greenwater River valley about 6 km.

When it encountered a narrow gorge of the White River at Mud Mountain that is only 300 m wide, the Osceola Mudflow spread out over glaciofluvial terraces of Vashon age that are up to 110 m above the White River (Fig. 7, A, section 3; and B). As it continued westward, the mudflow poured over terrace scarps to form a spectacular pair of falls (Fig. 7C). The upper fall would have formed an arc more than 6 km wide and more than 80 m high, and the second would have been more than 3 km wide and more than 110 m high.

In the lowland, the Osceola Mudflow completely choked the channel of the White River, which in pre-Osceola time followed the relatively confined valley of South Prairie Creek southwestward to join the Puyallup River at Orting, then flowed northwestward across the drift plain into the Green River drainage (Crandell, 1963b). When the White River reestablished normal flow, it flowed northwestward toward Auburn along the radically different course near the axis of the lahar lobe.

The Osceola entered the Duwamish and Puyallup embayments of Puget Sound via deltas at the mouths of the Green and Puyallup rivers (Fig. 1). Low gradients on the deltas caused the debris flow to pile up to thicknesses of more than 20 m near Auburn and Sumner (Dragovich et al., 1994). Deposits are generally present only in the subsurface in the Duwamish and Puyallup valleys. Wood-bearing, clayey, gravel-rich deposits at depths of 20 to 100 m northwest of Puyallup and north of Auburn show that the Osceola Mudflow retained its coherence and flowed more than 20 km under water.

**SEDIMENTOLOGY**

**Sediment-Size Analysis**

The entire Osceola Mudflow, including its hummocky facies, moved as a debris flow, the deposits of which mostly have greater than 5% clay (Table 4; Figs. 2 and 8). Notable exceptions with about 2% clay are samples from the base of normally graded axial facies and from valley-side facies (Figs. 8 and 9). As a proportion of the matrix (*sand + silt + clay*), clay is moderate to very large, 6% to 37% (Table 4).

The collapsing edifice apparently transformed to a debris avalanche then to a debris flow so quickly and completely that only a few large rock fragments survived intact to form hummocks. The hummocky facies is characterized by high silt and sand content (Table 4). It is interesting that samples from the hummocky facies have clay contents that range from 3.1% to 7.5% and from 7% to 12% of total *sand, silt, and clay* (Fig. 8; Table 4). Median diameter ranges from 1 to 32 mm, and sorting is slightly less than average (Fig. 8).

Three samples taken from valley-side facies near the upper limit of inundation have relatively large proportions of gravel and of *sand* to total *sand, silt, and clay* (Fig. 8; Table 4, nos. 3, 11, and 17); median diameters from about 4 mm to 12 mm; and slightly better sorting factors than average. A single sample from an intermediate position (Table 4, no. 10) also contains substantial *gravel* but considerably more *clay* than samples at the inundation limit and is thus more poorly sorted.

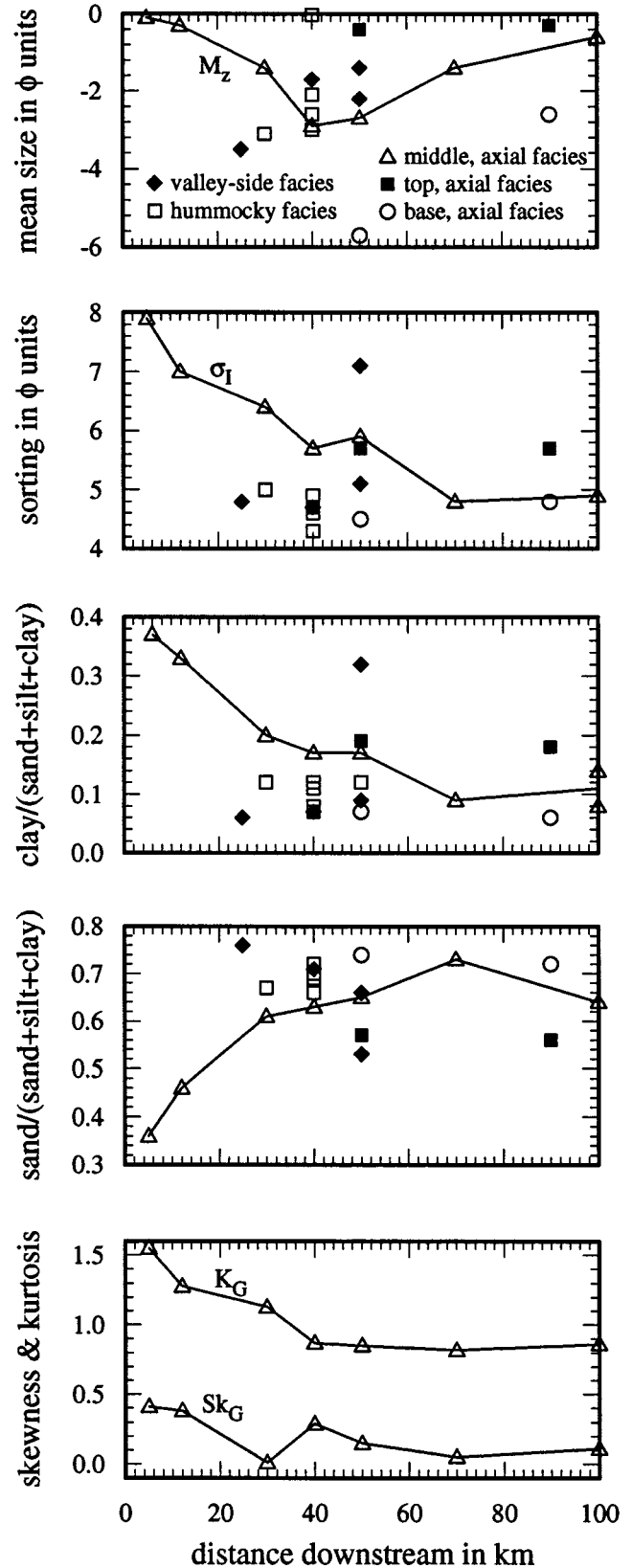


**Figure 8.** Graphs showing downstream trends in mean size, clay/(sand + silt + clay), sand/(sand + silt + clay), sorting, skewness, and kurtosis of sediment samples of the Osceola Mudflow.

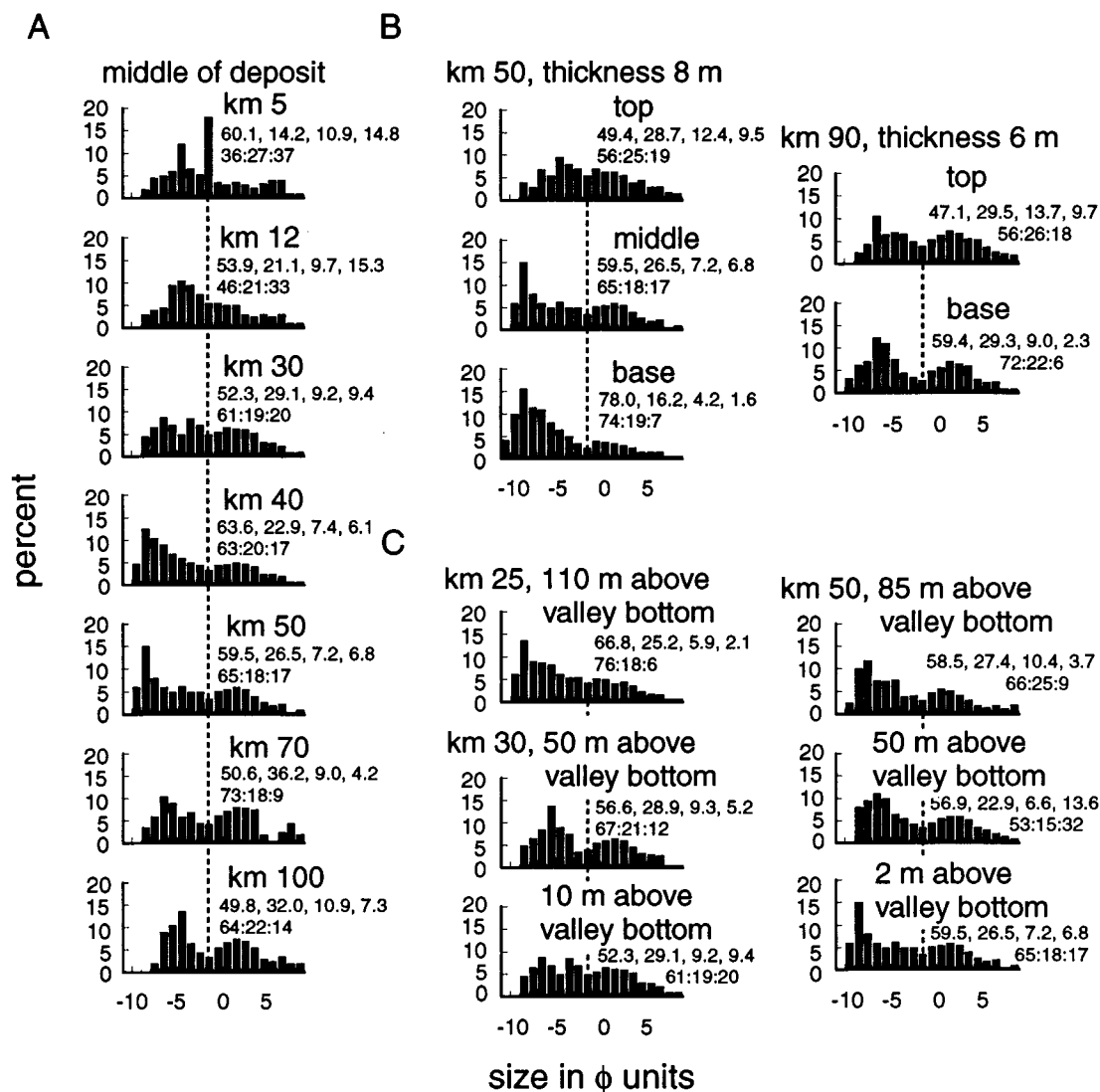


Figure 9. Histograms showing textural changes of samples of Osceola Mudflow. (A) Changes in axial facies with downstream distance, each sampled from the mid-thickness of deposit. (B) Changes in axial facies with stratigraphic position. (C) Changes with position in the valley. Percent of gravel, sand, silt, and clay and ratio of sand:silt:clay are given at the right of each histogram.

Progressive downstream changes in the >100 km course of the Osceola Mudflow correspond to streamwise textural changes in the axial facies (Fig. 8). Mean grain size ( $M_z$ ) increases from 1 mm at 5 km downstream to 8 mm at 50 km downstream and decreases to 2 mm at 100 km (Fig. 8). The corresponding sorting improves from 7.9 to 5.9 to 4.8  $\phi$  (Fig. 8). Initial values of sorting are anomalously high even for such poorly sorted deposits as debris flows. Initially poor sorting is caused by clay contents of up to 15% in addition to a complete spectrum of sand, silt, and gravel. Progressive downstream improvement in sorting results from incorporation of better sorted alluvial gravel and sand (see following section). There is, however, no apparent tendency toward a downstream transformation to lahar runoff flow. The downstream dilution of clay owing to incorporation of sand and gravel (Fig. 8) causes a corresponding decrease in skewness from slightly positive (excess fine material) to about zero and a change in kurtosis (peakedness) from 1.5 to 0.85 (Fig. 8).

Trends similar to those in the downstream direction can be seen from top to bottom of thick, normally graded, valley-fill outcrops. Two samples from a 6 m outcrop 90 km downstream, and three samples from an 8 m outcrop 50 km downstream, exhibit increased mean grain size and improved sorting from top to bottom (Fig. 9B). A downward increase in gravel and in sand/(sand + silt + clay) (Fig. 9) is typical of axial facies deposits.

Two samples, one from the proximal part (5 km from source) and one from the medial part (12 km from source) of the Osceola Mudflow, exhibit positive skewness owing to extended fine-grained tails and broad modes in the pebble-size class (Fig. 9A). A bimodal distribution of sediment sizes—one a sharp-peaked, coarse-gravel mode and the other a broad-peaked, sand mode (Fig. 9A)—develops and increases downstream. There is a similar increase in bimodality from top to bottom of normally graded deposits (Fig. 9B). Bimodal gravel and sand distributions also occur in the hummocky and valley-side facies (Fig. 9C).

Increased bimodality of downstream samples compared with proximal ones is interpreted to reflect progressive downstream erosion and incorporation of both sand and gravel. The node in bimodal samples falls between 1 and 8 mm and is typically centered at about 4 mm (Fig. 9). The dearth of 1–8 mm sediment could be a result of incorporation of two different populations of sediment, one dominantly coarse gravel and the other dominantly sand, neither one of which contains significant intermediate sediment. Another possibility is wholesale incorporation of sediment lacking in the 1–8-mm size class. Alluvium comprising mixtures of gravel and sand typically lacks sediment of this size class (e.g., Richardson, 1982), so that large-scale incorporation of alluvium may partly cause the 4 mm node.

### Bulking During Downstream Transportation

**Bulking Through Incorporation of Megaclasts.** Megaclasts (clasts 10 m or larger in diameter) generally consist of Mount Rainier andesite and are thus coherent fragments of the original edifice; however, some large fragments were derived from outcrops of bedrock along the path of the flow. Most megaclasts are observed only as hummocks, but at a few localities megaclasts can be seen in cross section. At least three of several hundred hummocks near Buck Creek are derived from the Tatoosh pluton, which crops out in the upper White River valley (Fiske et al., 1963), and are apparently fragments of bedrock or glacial erratics picked up by the flow then transported downstream. At Huckleberry Creek, 19 of 20 hummocks examined are Mount Rainier andesite, but one is composed of altered volcanoclastic rock of the Miocene Stevens Ridge Formation (Frizzell et al., 1984). The Stevens Ridge Formation crops out a few kilometres upstream in the Dalles narrows. A megaclast exposed in outcrop along Twin Creeks is formed entirely of unconsolidated alluvium, which is now internally deformed, with beds dipping 20%–40%. About 10 km farther downstream, near Scatter Creek, 14 of 15 hummocks examined are Mount Rainier andesite; one, which has a comparatively low profile, is composed entirely of loose cobble-rich alluvium. Three hummocks, 2 km downstream from Mud Mountain Dam, are all composed of glaciofluvial sediment. The hummocks appear on a high terrace, 8 km downstream from the easternmost (upvalley) outcrop of Vashon-age drift; the material in the hummocks is similar to, and was thus probably derived from, local kame-terrace deposits of Vashon age.

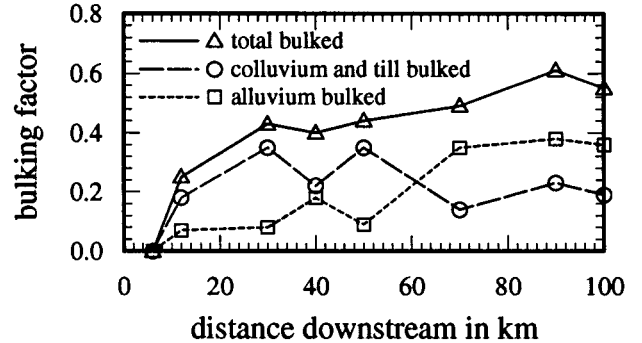
The Osceola Mudflow probably incorporated exotic megaclasts by undermining glacial erratics or bedrock outcrops situated on steep slopes in mountain valleys. Megaclasts of loose gravel within the deposit can be explained only by the undermining and wholesale incorporation of sediment during flowage. These huge gravel masses occur only close to their source areas; probably such incompetent masses break into separate pieces after transport of more than a few kilometres. Wholesale incorporation of gravel megaclasts into the flow is a likely source of some of the well-rounded pebbles, cobbles, and boulders that are abundant in the Osceola Mudflow.

**Bulking Through Incorporation of Gravel.** The Osceola Mudflow incorporated alluvium, colluvium, glacial drift, and bedrock by undercutting and wholesale incorporation of particles and by piecemeal erosion along the boundary layer. Abundant wood fragments and casts of wood fragments found in the Osceola Mudflow suggest a third mechanism by which particles might be incorporated. In its passage downstream, the lahar probably uprooted huge tracts of forest. Inspection of roots of fallen trees found in surrounding forests today indicates that considerable sediment is dragged up with the roots when the trees fall, and this mechanism could have contributed a significant volume of sediment to the lahar. Furthermore, uprooting of trees is apt to loosen underlying sediment and thus make it more susceptible to erosion.

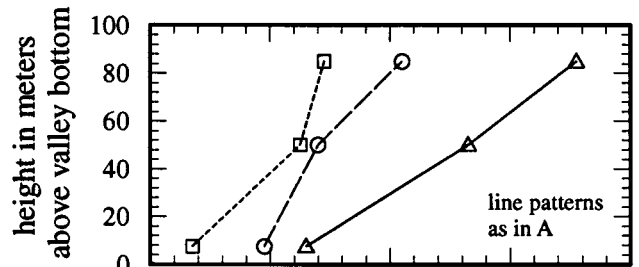
Bulking of clasts in the 16 to 32 mm size is best measured by the total bulking factor (*TBF*), which we use to measure the total proportion of particles incorporated into the flow by erosion at the boundary layer or incorporated by erosive undercutting, collapse, and dispersion. Particles that compose the original avalanche mass are almost entirely Mount Rainier andesite or altered andesite, and are angular to subrounded; thus, exotic lithologies and rounded particles were incorporated by the flow as it moved downstream.

Gravel particles found in the Osceola Mudflow can be classified into three groups on the basis of roundness and lithology. The susceptibility of particles to being rounded depends on particle size, so that the boundary between rounded and angular to subangular particles varies with size. The results of our study and those of Scott (1988) show that on a scale of roundness from 0 to 1, 0.4 serves as a good demarcation between subrounded

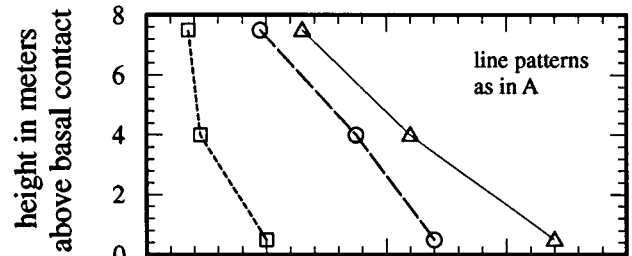
### A Bulking vs. distance downstream



### B km 50



### C km 50



### D km 90

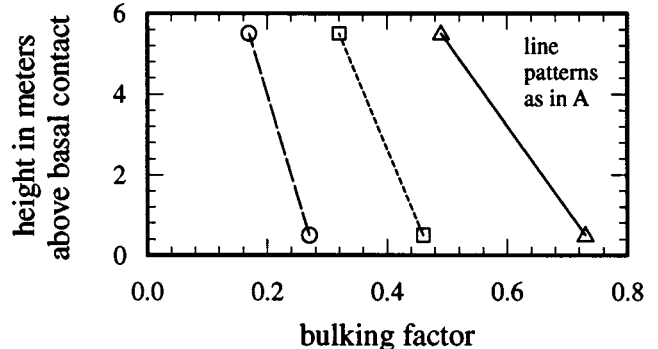
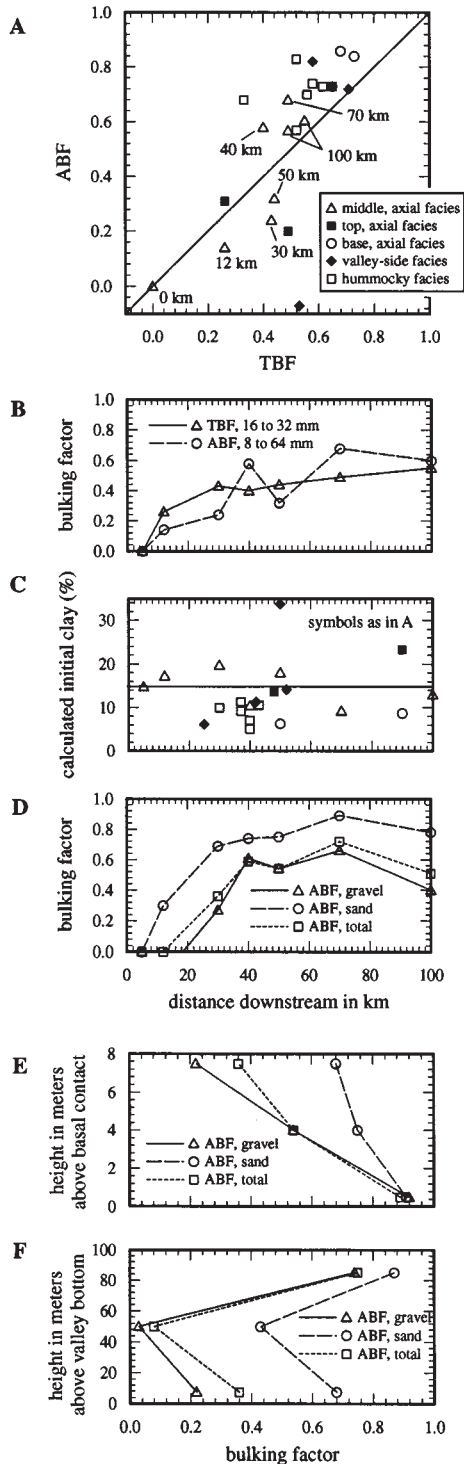


Figure 10. Graphs showing trends in bulking factor of 16–32 mm size class (A) versus distance downstream; (B) versus position in the valley 50 km downstream; (C) versus position in outcrop 50 km downstream; (D) versus position in outcrop 90 km downstream. Bulking factors are measured for axial facies in A, C, and D; and for both axial facies and valley-side facies in B. Solid lines show total gravel bulked (*TBF*), short dashed lines show rounded and subrounded alluvial gravel bulked (*LBF*), and long dashed lines show angular and subangular gravel bulked.



**Figure 11.** Graphs showing trends in bulking factor of 16–32 mm size class (A) versus distance downstream; (B) versus position in the valley 50 km downstream; (C) versus position in outcrop 50 km downstream; (D) versus position in outcrop 90 km downstream. Bulking factors are measured for axial facies in A, C, and D; and for both axial facies and valley-side facies in B. Solid lines show total gravel bulked (*TBF*), short dashed lines show rounded and subrounded alluvial gravel bulked (*LBF*), and long dashed lines show angular and subangular gravel bulked.

and rounded particles for the 16–32 mm size class. This implies that all particles having a roundness of 0.4 or greater are of alluvial or glaciofluvial origin. Furthermore, particles not of Mount Rainier provenance having a roundness of less than 0.4 derive from colluvium, till, or bedrock. Particles of Mount Rainier provenance having a roundness of less than 0.4 derive from the original avalanche mass.

The total bulking factor of the 16–32 mm size class for the Osceola Mudflow varies from 0 to 0.73 (Fig. 10). Samples from the proximal part of the deposit are unaffected by bulking, but those from the medial and distal parts show progressive downstream bulking. Samples from the middle stratigraphic level of axial facies deposits are appropriate “average” representatives of the Osceola Mudflow, because these fill deposits make up the greatest volume of debris at any particular place downstream. Total bulking represented by these samples increases with distance downstream. The proportion of angular particles bulked is greater than that of rounded ones between 10 and about 60 km downstream, but the proportion of rounded particles bulked predominates farther downstream (Fig. 10A). Thus colluvium, bedrock, and glacial till are the dominant sources of eroded particles in steep-sided valleys upstream from Greenwater, whereas alluvium and glaciofluvial deposits are the dominant sources downstream. In normally graded axial deposits, both bulking and the proportion of gravel-sized particles increase from top to bottom (Fig. 10, C and D). Bulking also increases with height above the valley bottom (Fig. 10B). It is interesting that outcrops of the hummocky facies, which are found relatively high in the valley, have large bulking factors ranging from 0.32 to 0.61 (Fig. 11A).

**Clay Content and Apparent Bulking and Debulking Factors.** An apparent bulking factor can be calculated for downstream samples if the following assumptions can be made: (1) an average initial clay content relative to other size fractions is that of the most proximal sample; (2) the material incorporated through erosion contains negligible clay; and (3) loss of particles through selective destruction or deposition is negligible. The apparent bulking factor (*ABF*) (derived in Data Repository<sup>1</sup>) is

$$ABF = 1 - \left( \frac{S_i}{C_i} \right) \left( \frac{C_f}{S_f} \right), \quad (1)$$

where *S* is any size fraction, *C* is the clay size fraction, *i* is a subscript referring to the initial fraction, and *f* is a subscript referring to the final fraction. The *ABF* must be positive. If the result is negative, then the size fraction may have been selectively deposited and an apparent debulking factor (*ADF*) (see Data Repository) may be calculated as

$$ADF = 1 - \left( \frac{C_i}{S_i} \right) \left( \frac{S_f}{C_f} \right). \quad (2)$$

The initial clay fraction, *C<sub>i</sub>*, and size fraction of interest, *S<sub>i</sub>*, are taken to be those of the most proximal sample, which, in this case, is the one collected from a distance of 5 km from source (Fig. 9A, 5 km; Table 4, no. 1). The final clay fraction, *C<sub>f</sub>*, and size fraction of interest, *S<sub>f</sub>*, are those of any other sample (Fig. 9; Table 4, no. 2–21). As an example, the *ABF* of sand for a sample 50 km downstream (Fig. 9A; no. 14; Table 4) is:

$$ABF = 1 - \left( \frac{0.142}{0.148} \right) \left( \frac{0.068}{0.265} \right) = 0.754. \quad (3)$$

The *TBF* is easy to measure for large particles, but difficult or impossible to measure for particles in the sand and silt size ranges. In contrast, the *ABF* is necessarily less accurate than a measured value, but is easy to de-

<sup>1</sup>GSA Data Repository item 9714 is available on request from Documents Secretary, GSA, P.O. Box 9140, Boulder, CO 80301. E-mail: editing@geosociety.org.

termine for any size class. It is also possible to calculate an  $ABF$  of all size classes together. This  $ABF_{total}$  is an estimate of the total amount of sediment bulked in a sample at any site, and hence the  $ABF_{total}$  of samples at all sites is an indication of the total erosion by the debris flow.

The  $ABF$ s of the 8–64 mm gravel give reasonable approximations of  $TBF$ s of 16–32 mm gravel from the middle of axial deposits, but those from the base of the axial facies and from valley-side and hummocky facies are more variable (Fig. 11, A and B). A plot of  $ABF$  versus  $TBF$  shows a definite trend with some scatter about a one-to-one correspondence (Fig. 11A).

One precondition for calculation of  $ABF$ s, the lack of clay-sized material in the sediment bulked, is satisfied where the eroded material is alluvium, talus, or bedrock, because these materials have little or no clay in them. Incorporated soil and glacial drift, to a lesser extent, may have a significant amount of clay. The results of this study suggest that clay-size material is a very minor component of the total bulked sediment.

A second precondition for the calculation of the  $ABF$  is a uniform clay content in the original avalanche mass. A survey of proximal deposits of the Osceola reveals that none was affected by bulking. Most of them appear to be rather uniform in texture, because of the very rapid mixing of the heterogeneous avalanche material. Nevertheless, there probably was some variability in the clay content in the original avalanche mass that would affect calculated bulking factors. Despite the variability of bulked material and especially of the source material,  $ABF$ s show remarkably good qualitative trends (Fig. 11B).

Replacing the  $ABF$  of a particular size class in equation 1 with the measured  $TBF$  of the size class and substituting the ratio of the size fraction to that of the clay fraction ( $C_i/S_i$ ) permits the initial ratio of clay to that size class ( $C/S_i$ ) to be calculated. The further assumption that the ratios of other size fractions are approximately that of the reference sample permits the initial clay contents for each sample to be estimated (Fig. 11C). Initial clay fractions estimated in this way vary from 0.05 to 0.34, but most range from 0.08 to 0.2. Of samples from the middle of valley-fill deposits, those nearer the source have larger calculated initial clay (CIC) fractions, and those farther downstream have smaller calculated initial clay fractions. Moreover, samples from stratigraphically higher parts of axial facies and, in one case, from an intermediate position on the valley side, have large calculated initial clay fractions, but generally samples from the valley-side facies and those from the hummocky facies have smaller-than-average calculated initial clay fractions. Samples from near the base of the axial facies also have small calculated initial clay fractions, only 0.06 to 0.08.

The  $ABF$  of each sample can be calculated, but a modified  $ABF$  ( $ABF'$ ) using the CIC fraction is probably more accurate. The  $ABF'$ s of the 8 to 64 mm size class calculated using the CIC fraction are the same as the  $TBF$ s of the 16 to 32 mm size class, and we infer that  $ABF'$ s of sand and gravel sizes are likely to approximate  $TBF$ s more closely than  $ABF$ s. The  $ABF'$ s are plotted in Figure 11, D, E, and F. The  $ABF'$ s of sand vary from 0 to 0.8 and those of total gravel vary from 0 to 0.8. The  $ABF'_{total}$  varies from 0 to about 0.7 and averages  $\approx 0.5$ .

The  $ABF'$  of sand and gravel increases downstream to about 50 km, beyond which there is a decrease, particularly in gravel (Fig. 11D). Corresponding with the decrease in  $ABF'$  between 50 and 100 km is a slight increase in  $TBF$  of gravel (Fig. 10D). Decreased  $ABF'$ s beyond 50 km suggest some upstream deposition of coarser clasts, particularly of gravel size, but increased  $TBF$  suggests the continued incorporation of foreign particles. Between 50 and 100 km downstream both erosion and deposition of sand and gravel are apparently important processes. As might be expected, the  $ABF'$ s of sand and gravel increase with depth in outcrops of graded axial-facies deposits (Fig. 11E); similarly, the  $ABF'$  of sand and gravel increases with greater height in the valley (Fig. 11F). Peak-flow debris (inundation-limit, valley-side deposits) have considerably larger

proportions of exotic sand and gravel owing to bulking than do the deposits of waning stage flows (Fig. 11F).

### Fabric

Clast fabric within the Osceola Mudflow was determined by measuring the long axes of clasts in the 32–64 mm size class at six localities (Fig. 12). Most particles in the Osceola are equant or of irregular shape, but a few particles have  $a$  axes significantly longer than  $b$  and  $c$  axes. We measured the long-axis orientation of prolate particles that had  $a$  axes at least 1.5 times those of the  $b$  and  $c$  axes and measured a suite of 25 or 40 clasts at each site. At four of the sites, we analyzed two or three suites of samples from a vertical sequence. Because most of the sites are on gently sloping terrain with bedding planes dipping  $0.5^\circ$  to  $7^\circ$ , the plots are not rotated to correct for dip.

The eigenvalue method of Mark (1973, 1974), used for three-dimensional analyses of the data, generates three perpendicular eigenvectors,  $V_1$ ,  $V_2$ , and  $V_3$ , and their significance levels in terms of the eigenvalues divided by the number of samples taken,  $S_1$ ,  $S_2$ , and  $S_3$  (Table 5). The eigenvectors,  $V_1$  and  $V_3$  are, respectively, the axes of maximum and minimum clustering of particle long axes (Mills, 1984; Major and Voight, 1986).

Deposits from near the base of normally graded deposits that are clast supported typically have a weak imbricate fabric (Fig. 12, 5B and 6B). The fabrics in the upper, matrix-rich part of thick, axial deposits indicate weak long-axis orientations transverse to the flow direction (Fig. 12, 5M and 6M), weak girdle fabrics with no preferred azimuthal direction (Fig. 12, 5T), or a strong alignment in the direction of flow (Fig. 12, 1B, 1M, 1T, 4B, 4T, and 6T). Clasts in deposits from steeper slopes commonly have strong alignment of their long axes in the inferred downslope direction of flow (Fig. 12, 1B, 1M, 1T, and 2M).

### Cataclasis and Abrasion

Clasts in the 16–32 mm size class, and especially those with partially stream-rounded surfaces, were examined for evidence of breakage (cataclasis) or abrasion during flow. Between 6% and 25% of the clasts show clear evidence of breakage. Broken clasts are most common in clast-supported basal parts of axial deposits and least common in the matrix-rich upper part of axial deposits. Broken clasts were also more common in deposits higher in the valley, especially those near inundation limits. The downstream increase in rounding of angular particles in the original avalanche mass suggests a progressive abrasion of gravel-sized particles. Overall cataclasis and rounding were substantial and comparable to those processes in the largest noncohesive lahar of 1980 at Mount St. Helens (Scott, 1988), despite the possible cushioning effects of the clay-rich matrix in the Osceola Mudflow.

### ORIGIN OF MASSIVE AND NORMALLY GRADED OSCEOLA DEPOSITS

It is common to infer that unstratified deposits like those of the Osceola Mudflow are emplaced en masse and that the deposits somehow reflect the nature of the flow as it passed (e.g., Johnson, 1970; Sparks, 1976), but the sedimentology of the massive, and in many places normally graded, Osceola Mudflow suggests that such an interpretation is too simplistic (Table 6). We suggest that Osceola deposits reflect the conditions at the time of deposition and that some deposits, like thick axial facies, may have been deposited incrementally over significant time intervals. Any interpretation of the Osceola Mudflow must account for the deposit characteristics listed in Table 6.

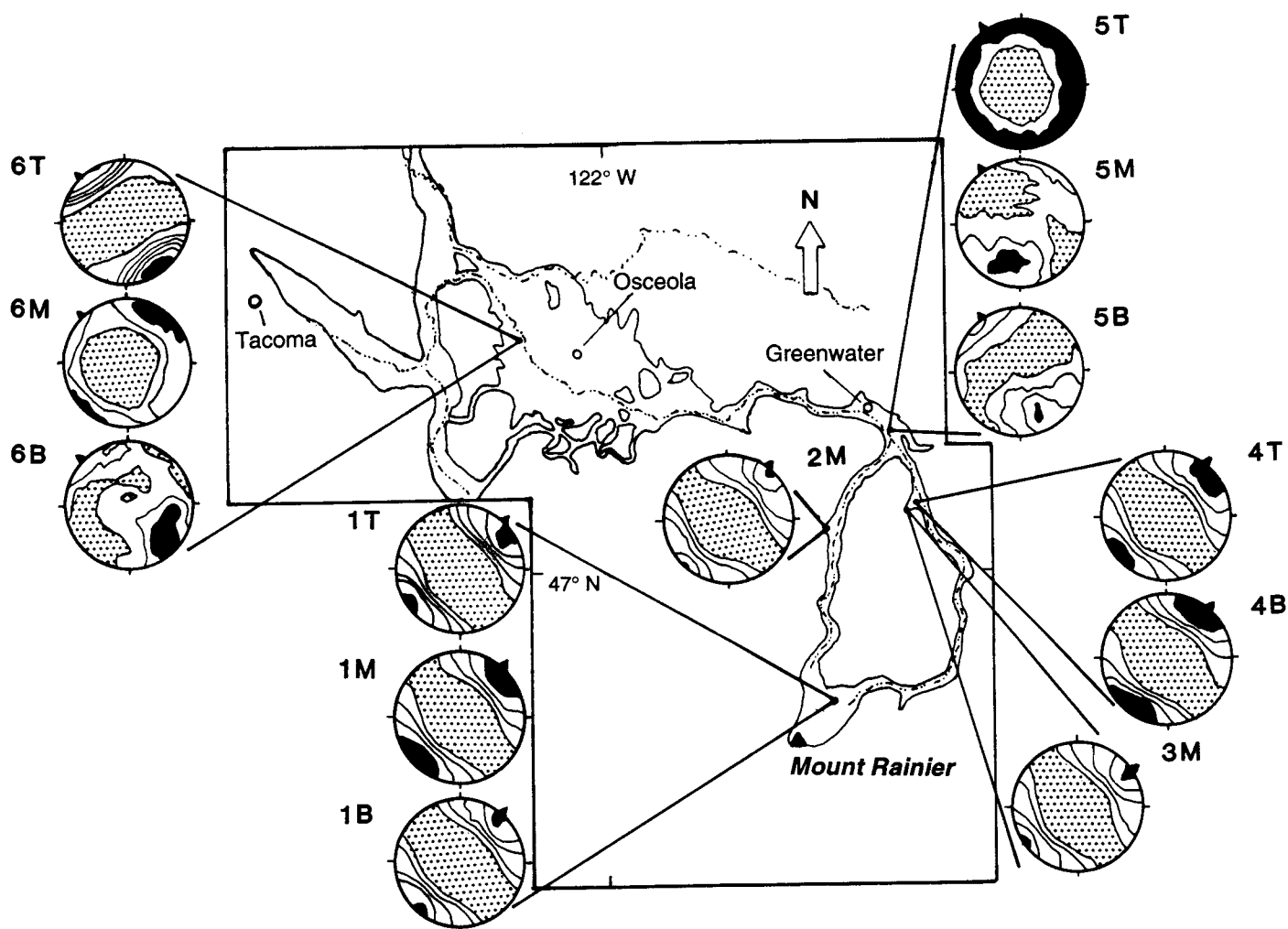


Figure 12. Lower hemisphere, equal-area projections of long axes of clasts measured in Osceola Mudflow ( $n = 25$  except  $n = 40$  at Greenwater site). Diagrams contoured using method of Kamb (1959), with contour intervals of two standard deviations. Arrow on equator indicates flow direction. T indicates plot is for top one third of deposit; M, middle one third; and B, basal one third.

### Why Osceola Deposits Are Massive

Massive deposits and the absence of stratification within vertical sequences, like those of the Osceola Mudflow, have traditionally been advanced as evidence of *en masse* deposition, but it is possible that incrementally accreted debris that is very poorly sorted and contains sparse elongate particles might appear to be massive. Experiments suggest a mechanism whereby the deposits of the Osceola Mudflow could have been emplaced by incremental accretion and yet not be stratified. Deposits of experimental debris flows in a flume 90 m long and 2 m wide accrete incrementally but are massive and unstratified (Major, 1996). In laboratory experiments with bimodal and multimodal mixtures of dry sand and beads, Vallance (1994b) observed that the sand comes to rest from the bottom up as it moves from steep slopes onto gentle ones. A zone of creeping flow forms between the static sand below and rapidly moving sand above as aggradation proceeds. The creeping layers present during accretion of the sand appear to destroy stratification in the resulting deposits.

Several features of thick massive Osceola deposits suggest that they accreted incrementally despite the lack of apparent stratification (Table 6). Imbricate fabrics in the basal part of thick, normally graded, axial deposits suggest piecemeal deposition of these particles. Strong parallel alignment

of elongate particles in other parts of the deposits (Fig. 12) are consistent with piecemeal deposition of particles from a flow with significant shear-strain rate and a basal boundary that migrates upward. Compositional zoning of thick axial deposits suggests incremental accretion of a compositionally zoned flow (e.g., Fisher, 1966; Branney and Kokelaar, 1992). Layers of creeping debris several centimeters to several meters thick that might have formed during accretion of Osceola debris could have blurred and destroyed incipient stratification in massive Osceola deposits, even thick normally graded ones. We infer that the massive appearance of these deposits is caused by a combination of accretion and creep rather than by the *en masse* deposition of a massive flow that is more commonly assumed (e.g., Johnson, 1970; Fisher and Schmincke, 1984).

### Importance of Gravitational Settling in the Genesis of Normally Graded Bedding

Normally, grading is common in clay-rich debris-flow deposits and inverse grading is rare (Crandell, 1971; Vallance, 1994a; this paper). Segregation by gravitational settling in a debris flow depends on large particles migrating downward faster than small ones in matrix-rich debris. Matrix slurry strength enhances the segregation, because particles smaller than a

OSCEOLA MUDFLOW, MOUNT RAINIER

TABLE 5. SUMMARY OF EIGENVALUE ANALYSES OF CLAST FABRIC FOR THE OSCEOLA MUDFLOW

Sample number	Facies	Local slope	Flow direction	Number measured	V <sub>1</sub> Azimuth	V <sub>1</sub> Dip	S <sub>1</sub>	V <sub>3</sub> Azimuth	V <sub>3</sub> Dip	S <sub>3</sub>
1T	Axial	4°	45°	25	50°	20°	.817	232°	70°	.067
1M	Axial	4°	45°	25	48°	27°	.715	218°	62°	.115
1B	Axial	4°	45°	25	46°	28°	.721	315°	3°	.117
2M	Valley-side	7°	55°	25	50°	21°	.686	183°	48°	.116
3M	Valley-side	1.4°	50°	25	53°	21°	.759	250°	68°	.043
4T	Axial	1.2°	45°	25	38°	24°	.734	182°	61°	.103
4B	Axial	1.2°	45°	25	47°	24°	.673	194°	62°	.146
5T	Axial	0.6°	335°	40	74°	7°	.482	255°	83°	.085
5M	Axial	0.6°	335°	40	208°	26°	.534	316°	30°	.165
5B	Axial	0.6°	335°	40	150°	24°	.589	28°	49°	.172
6T	Axial	0.5°	320°	40	148°	6°	.789	307°	84°	.050
6M	Axial	0.5°	320°	40	44°	12°	.499	245°	78°	.098
6B	Axial	0.5°	320°	40	133°	22°	.525	235°	28°	.198

Note: The critical values of S<sub>1</sub> and S<sub>3</sub> at the 0.05 significance level are: S<sub>1</sub> = 0.473 and S<sub>3</sub> = 0.203 for N = 40 and S<sub>1</sub> = 0.515 and S<sub>3</sub> = 0.181 for N = 25 (Mark, 1973, 1974). Calculated values of S<sub>1</sub> greater than the critical value and S<sub>3</sub> less than the critical value are significant with 95% confidence.

TABLE 6. SUMMARY OF CHARACTERISTICS OF OSCEOLA MUDFLOW DEPOSITS AND THEIR INFERRED IMPLICATIONS REGARDING EMPLACEMENT AND FLOW CONDITIONS

Deposit characteristics	Consistent with			
	En masse emplacement	Incremental emplacement	Longitudinally graded flow	Vertically graded flow
1 The deposits appear to be massive and unstratified.	Y	Y*	Y	Y
2 Despite their massive appearance, most deposits show strong alignment of elongate clasts parallel to flow directions or imbrication of elongate clasts in upstream directions.	N	Y	Y	Y
3 Peak flow depths in mountain valleys (typically 90 to 150 m) are five or more times greater than the thickest deposits.	N*	Y	Y	Y
4 Axial deposits thicker than about 1.5 m commonly are normally graded, but axial deposits less than about 1.5 m, valley-side deposits, and hummocky deposits commonly are ungraded.	Y	Y	Y	N
5 The largest clasts, boulders and cobbles, are most common at the base of normally graded deposits, but also occur at or near the tops of such deposits.	Y	Y	Y	N*
6 Normally graded deposits are also normally graded with respect to sand/(sand+silt+clay).	Y	Y	Y	N*
7 The upward decrease of gravel and sand/(sand+silt+clay) in normally graded deposits corresponds with a decrease in exotic gravel and sand incorporated through erosion.	N*	Y	Y	N*
8 A similar decrease in gravel and sand/(sand+silt+clay) from inundation limit to valley bottom also corresponds to a decrease in exotic gravel and sand bulked. There are also greater proportions of alluvial cobbles in inundation-limit deposits than in deposits from places lower in the valley.	N*	Y	Y	N*
9 Mount Rainier boulders and megaclasts are common near the inundation limit.	Y	Y	Y	N
10 The proportion of gravel-size particles in deposits is high, ranging from 40% to 78% and averaging 56%. Gravel particles broken during flow are common.	Y	Y	Y	N†

Note: Y means consistent; N means not consistent.

\*See discussion in text.

†A high proportion of gravel particles will hinder gravitational settling of large particles and can cause inverse segregation if shear strain rate is not zero.

critical diameter cannot settle. If a normally segregated flow stops rapidly enough, the resulting deposit will be normally graded. This scenario is often suggested to explain normal grading in debris flows (e.g., Fisher and

Schmincke, 1984). However, it is not clear whether such a mechanism can work effectively in a medium, like the Osceola Mudflow, that has a large solids content (>60% by volume) and large proportions of gravel

(40%–78%; 56% average), partly because a large quantity of solid particles may hinder the settling (Phillips and Davies, 1991), but mainly because of the opposing tendency of small particles to percolate downward and displace large ones upward in regions with large proportions of gravel and nonzero shear strain rates (e.g., Middleton, 1970; Vallance, 1994b).

Not only are thick deposits of the Osceola Mudflow normally graded with respect to cobbles and boulders, but they are also normally graded with respect to sand. The proportion of sand in the matrix (*sand + silt + clay*) is greater near the base than near the top of axial fill deposits (Table 4, nos. 13–15 and 19–20). Because of having small or zero settling velocities in the clayey, sediment-rich Osceola matrix, particles as small as sand could not have settled relative to smaller matrix particles. Furthermore, some particles in all size classes, including huge boulders, are present in the upper parts of normally graded axial deposits. The presence of such large particles at the top and increased concentrations of sand-sized particles at the base of normally graded deposits suggests that the mechanism of gravitational settling cannot wholly explain normal grading in the Osceola Mudflow, except possibly as it contributes to coarse-tail grading of large boulder- and cobble-sized clasts.

**Normal Grading by Incremental Deposition From a Longitudinally Segregated Flow**

Systematic variation of grain size and composition within and among deposits suggests that the Osceola Mudflow was longitudinally segregated such that it was coarser grained, better sorted, and contained more exotic

particles at its front than at its tail. Although little can be inferred about the rising stage of the Osceola Mudflow, inundation limit deposits were deposited at peak inundation, and deposits successively lower on valley sides were deposited during receding flow. Deposits near inundation limits show large proportions of exotic clasts, particularly gravel-size alluvium (Figs. 10B and 11F). The presence of gravel-size alluvium indicates thorough vertical mixing of exotic particles at the time of peak inundation because alluvium is not present on valley sides and must have migrated about 100 m upward from valley bottoms. Deposits lower on valley sides show progressively decreasing exotic fractions that indicate changes in the composition of the flow as it receded. The large to moderate proportion of alluvial particles at progressively falling stages (Fig. 10B) suggests continuing vertical mixing at successive times because these particles also had to migrate upward tens of meters from valley bottoms. We infer that inundation-limit deposits, hummocky facies deposits, and the basal parts of thick normally graded axial facies came from the same part of the flow wave because they are similarly rich in exotic sand and gravel and poor in clay. These parts of the Osceola Mudflow were apparently emplaced first, probably at or shortly after peak flow. Similarly, deposits progressively lower on valley sides and higher in normally graded valley-bottom deposits show diminishing exotic fractions and increasing clay fractions. We infer that these parts of the Osceola came from falling stages of the flow and were emplaced at successively later times.

A schematic hydrograph of a debris flow (Fig. 13) shows how incremental deposition of a longitudinally segregated flow could produce normally graded deposits. Depending on local conditions at any point in the

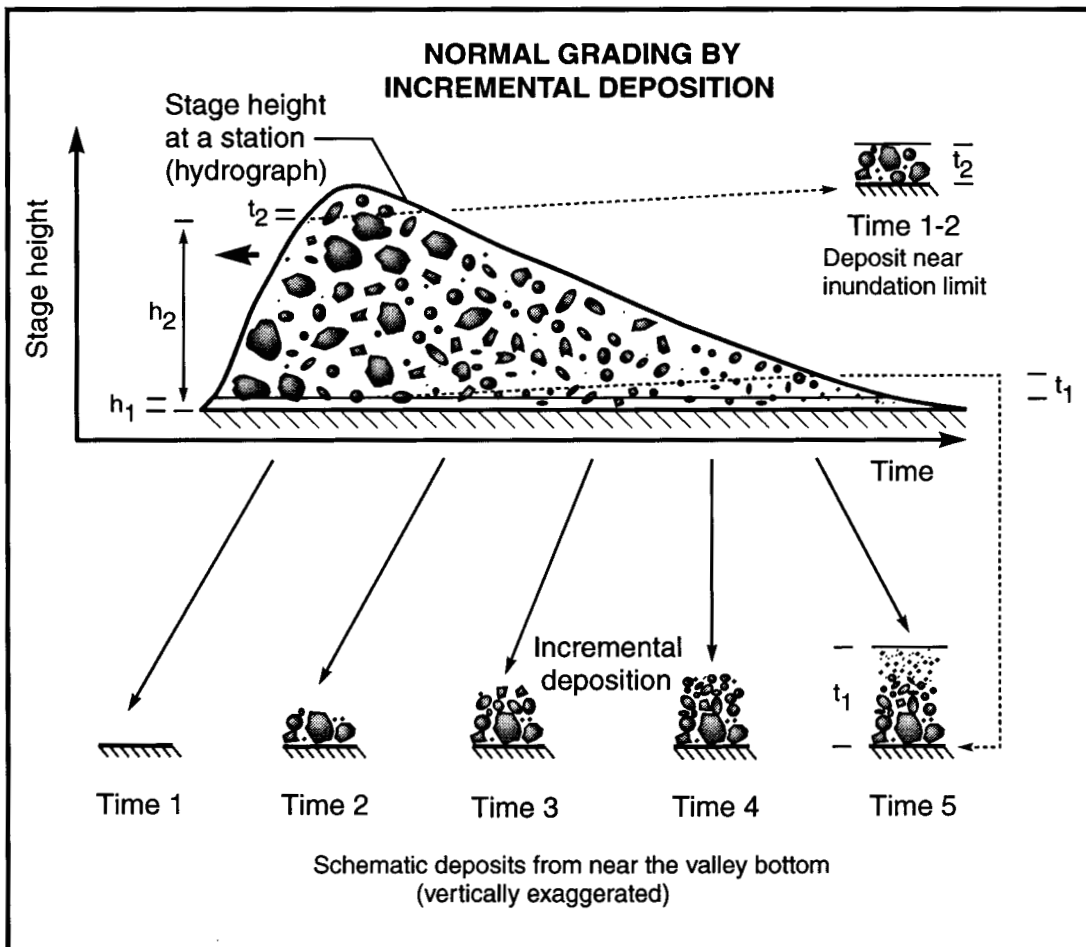


Figure 13. Schematic diagram of stage height versus time (hydrograph) for mass flow at point in bottom of valley, and depositional sequence of flow illustrating incremental-deposition model for explaining normal grading. Deposition illustrated for two stations 1 and 2 at heights  $h_1$  and  $h_2$  above valley bottom and with ultimate thicknesses  $t_1$  and  $t_2$ . Short dashed lines through hydrograph indicate uniform incremental deposition. Sense of motion of mass flow is to left. See text for explanation.

valley at any time, the debris flow may erode its base, deposit debris, or neither. Short dashed lines having positive slopes through the hydrograph, which can be thought of as deposition lines, illustrate steady incremental deposition in Figure 13. For a position near the valley bottom, steady incremental deposition would produce the depositional sequence illustrated by times 1 through 5 (Fig. 13). The initial part of the flow is enriched in gravel and has a sandy matrix; therefore the initial deposits (time 2, Fig. 13) are coarse grained. As the flow progresses, it becomes finer grained and its matrix becomes less sandy. With continuing aggradation, the deposit fines upward (times 3 and 4) until the stage height finally drops below the level of the deposit and deposition ceases (time 5). Because axial deposits are emplaced in the main channel of the flow, the onset of deposition there probably lags that at inundation limits (times 1 and 2).

At a site near the inundation limit, deposition would occur very rapidly because there the inundation limit is only a little higher than remnants of the deposit. However, the deposit is ungraded because the flow is at or above this stage only briefly, and the change in grain size longitudinally during this short interval is small (Fig. 13, times 1 and 2). The presence of normally graded deposits at positions lower in the valley and their absence at the inundation limit provide a check on the incremental deposition model of normal grading. Deposits of the Osceola Mudflow show such a distribution.

An important precondition in support of the incremental-aggradation hypothesis—that of longitudinal segregation of the flow wave—is also consistent with the sedimentological characteristics of the Osceola Mudflow illustrated in Figures 8 through 11 and listed in Table 6. As it moved downstream the Osceola Mudflow incorporated huge quantities of exotic sand and gravel. Because the bulked sediment is mostly sand and gravel from alluvium, colluvium, and glacial drift, it is coarser grained and better sorted than the original clay-rich debris of the Osceola Mudflow. The most erosive part of the flow would have occurred during waxing flow and peak inundation. Therefore, the first stage of the lahar would have been enriched in exotic sand and gravel in addition to being coarser grained and better sorted. If incremental accretion began with the passing of peak flow, then the initial, coarser-grained, better-sorted debris would have been deposited initially at inundation limits and in favorable sites in valley bottoms and on valley sides. Later, as it waned, the flow would have deposited debris less enriched in well-sorted, coarse-grained, exotic sand and gravel at sites lower on valley sides and stratigraphically higher in normally graded, axial sequences. These predictions match the deposit characteristics of the Osceola Mudflow (Table 6).

Steady uniform incremental accretion implied by Figure 13 is an overly simplistic model for a naturally occurring debris flow like the Osceola Mudflow. Erosion and deposition by the Osceola Mudflow probably depended on local conditions at a site and on conditions with respect to position in the valley. During rising flow, erosion was strongest, undermining steep banks and slopes, incorporating these masses as they slid into the flow, and ripping up trees. In many places, especially lowlands and valley bottoms, the Osceola Mudflow overlies complete soil profiles or tephra sequences, suggesting that it was very erosive in some places but completely passive in others. This suggests that erosion probably proceeded in sudden spurts as steep slopes were undermined then incorporated into the flow, and that piecemeal erosion, especially on gentle slopes, was less important. Periods of deposition were also variable and probably were of longer duration in areas near valley bottoms and of shorter duration near inundation limits.

There is no reason to assume that deposition of the Osceola Mudflow at any site was uniform. Deposition at some sites may have begun slowly at first, then proceeded more rapidly during the waning stages of flow. Some deposits near inundation limits and distal margins may have been emplaced very rapidly. At some sites, there may have been alternating periods of deposition and erosion. Because of changing flow conditions, debris that came to rest at the base of the flow might have begun to creep forward

again in a way somewhat analogous to bedload transportation during floods in river systems. If the Osceola hydrograph were characterized by multiple peaks rather than one sharp peak as illustrated in Figure 13, then debris at the base of some sections may have alternately crept forward and halted several times.

## GENESIS OF THE COHESIVE DEBRIS-FLOW WAVE

The initial avalanche mass of the Osceola Mudflow apparently homogenized by the time it arrived at Steamboat Prow, about 2 km from its source; however, estimates of the original clay content of the deposits suggest that the original avalanche front was richer in gravel and sand than the more clay-rich following parts and that subsequent addition of the huge amounts of exotic gravel and sand at the flow front enhanced longitudinal segregation of the flow as it moved down valley. Calculated initial clay contents (Fig. 11C) suggest that deposits from near inundation limits, from hummocky deposits, and from the base of thick valley-fill deposits were initially less clay rich and hence more sandy. These deposits must have been derived from the peak-flow wave as it moved downstream. The initial peak-flow wave was probably derived from the outer, less hydrothermally altered and hence less clay-rich, segment of the avalanche mass. Large calculated-initial-clay contents of deposits from the upper parts of axial deposits, from intermediate positions on the valley sides, and from valley bottoms closer to Mount Rainier suggest that these portions of the deposit are derived from the more intensely hydrothermally altered, clay-rich, interior segments of the avalanche mass. These portions of the avalanche would have initially formed the more clay-rich trailing part of the debris flow. In the previous section we showed that the front of the flow became enriched in exotic sand and gravel and hence coarser grained and better sorted relative to the following flow; here we suggest that the initial flow may also have started coarser grained at its front.

A possible scenario consistent with these interpretations is that the Osceola avalanche began with a succession of several slide blocks much as did the 1980 Mount St. Helens debris avalanche, but unlike the Mount St. Helens avalanche the blocks homogenized rapidly as they traveled downslope. The first slide block would have included a large proportion of fresh Mount Rainier andesite. Because fresh rock is more competent than altered rock, the first block probably became less completely homogenized as it transformed and flowed downstream. If this interpretation is correct, the first slide block would probably have been the source of the hummocky facies found on high terraces and in tributary valleys as far downstream as the Cascade Range mountain front. It may also have been the source of hummocky debris buried 10 to 20 m below more clay-rich Osceola debris in the Greenwater area. Successive slide blocks would have sliced more deeply into the core of the edifice and presumably more deeply into preexisting, clay-rich hydrothermally altered rocks. These blocks followed the initial hummock-bearing debris, but eventually flowed over and beyond it. The Osceola sector collapse began with several slide blocks or just one, but all of the initial slide mass apparently contained enough weak, hydrothermally altered rock and dispersed water to homogenize and begin behaving as a debris flow within 2 km of its source.

## HAZARD IMPLICATIONS

The Osceola Mudflow began as a sector collapse but has features more typical of a debris flow than of a debris avalanche. Ui (1989) suggested that hummocks are definitively characteristic of debris-avalanche deposits; however, the Osceola Mudflow has nearly flat surfaces and includes hummocks, yet behaved as a cohesive debris flow even in proximal areas. Most cohesive debris flows at stratovolcanoes begin as sector collapses, so their deposits have features of both debris avalanches and debris flows (Cran-

dell, 1989; Scott et al., 1992; Carrasco-Núñez et al., 1993; Vallance, 1994a; 1994b). Furthermore, many debris avalanches show gradations from irregular hummocky surfaces in axial and proximal areas to flat lahar-like surfaces in marginal and distal areas (Palmer et al., 1991). The results of this study and those just listed suggest a complete gradation in characteristics between those of cohesive lahars and those of debris avalanches in deposits originating as sector collapses.

Empirically, we observe that the presence of large volumes of clay-rich rock not only increases the likelihood of edifice collapse, but also increases the likelihood that the collapsing rock will disintegrate and transform into a debris flow rather than a debris avalanche. Abundant clay increases porosity, and increased pore-water content may further destabilize the altered rock, thus making it more susceptible to slope failure. Furthermore, clay-rich rock provides a ready source of the widely dispersed, abundant water necessary for the transformation of an avalanche into a debris flow. The collapses of hydrothermally altered rock at Mounts Baker, Rainier, and Adams during the Holocene typically formed debris flows rather than debris avalanches (Crandell, 1971, 1989; Hyde and Crandell, 1978; Frank, 1983; Scott et al., 1992; Vallance, 1994a).

Debris flows and debris avalanches are potential hazards at most strato-volcanoes, but the severity of hazard from noncohesive debris flows, cohesive debris flows, and debris avalanches differs because of their differing origins and behavior. Cohesive lahars like the Osceola generally begin when avalanches of clay-rich, hydrothermally altered rock, containing considerable water, transform to debris flows (Scott et al., 1992; Carrasco-Núñez et al., 1993; Vallance, 1994a). Debris avalanches have similar origins and comparable sizes, yet, because they contain less clay-rich rock and therefore less water, do not transform to debris flow. Cohesive debris flows are roughly twice as mobile in terms of their ratio of travel distance (length,  $L$ ) to vertical drop (height,  $H$ ) ( $L/H$ ) and may spread over areas one to ten times larger than debris avalanches having similar volume. In contrast, noncohesive debris flows generally begin when water from a crater lake, torrential rain, or rapidly melted snow and ice mixes with loose volcanoclastic debris (e.g., Pierson, 1985; Scott, 1988). Cohesive and noncohesive lahars may both have very long runouts, but cohesive lahars tend to be more voluminous and cover larger areas than noncohesive lahars (Fig. 14). Empirically, there is a strong correlation between volume and area for cohesive and noncohesive lahars (Fig. 14A). This relationship is potentially useful in hazards assessments because it allows an estimate of area covered to be made for any lahar of given volume.

The ratio of vertical drop to travel distance ( $H/L$ ) has been used to anticipate the maximum runout of future debris avalanches (Schuster and Crandell, 1984; Siebert et al., 1987; Crandell, 1989); however, the method should be used with great caution, because transformation of the avalanche to debris flow is possible. The  $H/L$  method of estimating avalanche runout is not straightforward, because  $H/L$  tends to decrease with increase in volume (Fig. 14B). Schuster and Crandell (1984) proposed an  $H/L$  of 0.075 and Siebert et al. (1987) proposed a value of 0.05 for estimating the maximum runout of debris avalanches. The Osceola Mudflow, however, has an  $H/L$  of 0.039 (0.046, from center of mass to center of mass). The Osceola and several other cohesive lahars are roughly two to five times more mobile than comparably sized volcanic debris avalanches (Fig. 14B; recall that the inverse of  $H/L$  is mobility).

The Osceola Mudflow is the largest lahar that occurred at Mount Rainier during the Holocene, so it can be used as a model of the behavior of the maximum-sized cohesive lahar that might occur in other valleys at Mount Rainier or in valleys at other volcanoes with large volumes of hydrothermally altered rock, like Mounts Adams and Baker. Because the maximum stage height and cross-sectional area of the Osceola remain relatively constant between 10 km from Mount Rainier and the Puget Sound lowland (Fig. 7), a similar inundation limit for the design-case maximum lahar can

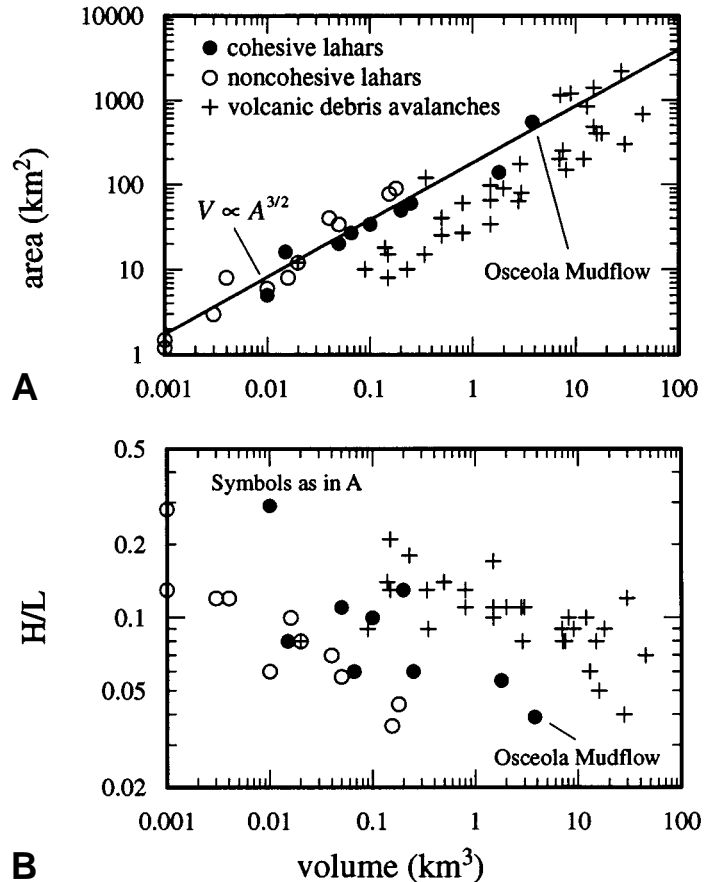


**Figure 14.** Graphs of area versus volume (A) and  $H/L$  (fall height / runout) versus volume (B) for cohesive lahars, noncohesive lahars, and volcanic debris avalanches. Data are from Siebert and others (1987) for volcanic debris avalanches; from Crandell (1971), Hyde and Crandell (1978), Scott et al. (1992), Carrasco-Núñez et al. (1993), and Vallance (1994a) for cohesive lahars; and from Pierson (1985), Major and Voight (1986), Ostercamp et al. (1988) and Scott (1988) for noncohesive lahars.

be applied in other confined valleys by assuming equal-area cross sections. The design-case inundation limit depends on the assumptions that valleys have similar shape, roughness, and long profile, and that discharge at any distance downstream remains constant. Upon reaching the Puget Sound lowland, the Osceola Mudflow spread widely (Fig. 1). We approach the problem of flow spreading in lowlands by assuming that the design-case lahar would spread across a similar area. The maximum design-case lahar at Mount Rainier is tentatively assigned a recurrence interval of 10 000 yr (Scott et al., 1995). Scott et al. (1995) and Scott and Vallance (1995) modeled similar smaller design-case lahars and assigned shorter recurrences to them on the basis of Holocene stratigraphy at Mount Rainier. The areas covered by such lahars in unknown valleys can be estimated using the relationship between area and volume illustrated in Figure 14. This design-case approach requires detailed stratigraphy and inundation-limit mapping at a volcano, but is a better way to assess the potential hazard of a sector collapse that could transform into a cohesive lahar than the  $H/L$  approach.

To assess potential consequences of sector collapse, an important issue is whether the avalanching debris will transform into a lahar or behave as debris avalanche, because the mobilities differ. A large volume of hydrothermally altered rock within the volcano not only increases the poten-

tial for sector collapse because the altered rock is less competent, but also increases its water content because fine-grained secondary material like clay decreases the permeability and increases the porosity of the rock. If the avalanching debris contains enough water, it will readily transform to a debris flow. Thus, the presence of large volumes of hydrothermally altered rock at an erupting volcano greatly enhances the risk from cohesive lahars.

## ACKNOWLEDGMENTS

The work was supported by the Water Resources Division of the U.S. Geological Survey at the Cascades Volcano Observatory. We greatly benefited from discussions with Rocky Crandell, Pat Pringle, and Joe Dragovich, and from the careful reviews of Rocky Crandell, Don Swanson, Vince Neall, and Kelin Whipple. We appreciate the efforts of Dan Gooding in overcoming the difficulties involved in sediment-size analyses of extremely clay rich, poorly sorted debris from the Osceola Mudflow. We thank Chris Janda for drafting several of the figures. We dedicate this to the memory of our imaginative and innovative friend, Dick Janda.

## REFERENCES CITED

- Bacon, C. R., 1983, Eruptive history of Mount Mazama and Crater Lake caldera, Cascade Range, USA: *Journal of Volcanology and Geophysical Research*, v. 18, p. 57–115.
- Beverage, J. P., and Culbertson, J. K., 1964, Hyperconcentrations of suspended sediment: *American Society of Civil Engineers Proceedings, Journal of the Hydraulics Division*, v. 90, p. 117–128.
- Branney, M. J., and Kokelaar, P., 1992, A reappraisal of ignimbrite emplacement: Progressive aggradation and changes from particulate to non-particulate flow during emplacement of high-grade ignimbrite: *Bulletin of Volcanology*, v. 54, p. 504–520.
- Carrasco-Núñez, G., Vallance, J. W., and Rose, W. I., 1993, A voluminous avalanche-induced lahar from Citlaltepétl volcano, Mexico: Implications for hazard assessment: *Journal of Volcanology and Geophysical Research*, v. 59, p. 35–46.
- Coombs, H. A., 1936, The geology of Mount Rainier National Park: *Washington University Publications in Geology*, v. 3, p. 131–212.
- Crandell, D. R., 1963a, Paradise debris flow at Mount Rainier: *in Short papers in geology and hydrology*, U.S. Geological Survey Professional Paper 475-B, p. 135–139.
- Crandell, D. R., 1963b, Surficial geology and geomorphology of the Lake Tapps quadrangle, Washington: U.S. Geological Survey Professional Paper 388-A, 84 p.
- Crandell, D. R., 1969, Surficial geology of Mount Rainier National Park, Washington: U.S. Geological Survey Bulletin 1288, 41 p.
- Crandell, D. R., 1971, Postglacial lahars from Mount Rainier volcano, Washington: U.S. Geological Survey Professional Paper 677, 75 p.
- Crandell, D. R., 1989, Gigantic debris avalanche of Pleistocene age from ancestral Mount Shasta volcano, California, and debris-avalanche hazard zonation: U.S. Geological Survey Bulletin 1861, 32 p.
- Crandell, D. R., and Miller, R. D., 1974, Quaternary stratigraphy and extent of glaciation in the Mount Rainier region, Washington: U.S. Geological Survey Professional Paper 847, 59 p.
- Crandell, D. R., and Waldron, H. H., 1956, A recent volcanic mudflow of exceptional dimensions from Mount Rainier, Washington: *American Journal of Science*, v. 254, p. 349–362.
- Dragovich, J., Pringle, P. T., and Walsh, T. J., 1994, Extent and geometry of the mid-Holocene Osceola Mudflow in the Puget Sound Lowland—Implications for Holocene sedimentation and paleogeography: *Washington Geology*, v. 22, no. 3, p. 3–26.
- Driedger, C. L., and Kennard, P. M., 1986, Ice volumes on Cascade volcanoes: Mount Rainier, Mount Hood, Three Sisters, and Mount Shasta: U.S. Geological Survey Professional Paper 1365, 28 p.
- Fisher, R. V., 1966, Mechanism of deposition from pyroclastic flows: *American Journal of Science*, v. 264, p. 350–363.
- Fisher, R. V., and Schmincke, H. U., 1984, *Pyroclastic rocks*: Berlin, Springer-Verlag, 472 p.
- Fiske, R. S., Hopson, C.A., and Waters, A. C., 1963, *Geology of Mount Rainier National Park*, Washington: U.S. Geological Survey Professional Paper 444, 93 p.
- Folk, R. L., 1980, *Petrology of sedimentary rocks*: Austin, Texas, Hemphill, 182 p.
- Frank, D., 1983, Origin, distribution, and rapid removal of hydrothermally formed clay at Mount Baker, Washington: U.S. Geological Survey Professional Paper 1022-E, 131 p.
- Frank, D., 1985, Hydrothermal processes at Mount Rainier [Ph.D. dissert.]: Seattle, University of Washington, 195 p.
- Frank, D., 1995, Surficial extent and conceptual model of hydrothermal system at Mount Rainier, Washington: *Journal of Volcanology and Geothermal Research*, v. 65, p. 51–80.
- Frizzell, V.A., Jr., Tabor, R. W., Booth, D. B., Ort, K. M., and Waitt, R. B., 1984, Preliminary geologic map of the Snoqualmie Pass quadrangle, Washington: U.S. Geological Survey Open-File Map 84-693, scale 1:100 000.
- Hyde, J., and Crandell, D., 1978, Postglacial volcanic deposits at Mount Baker, Washington, and potential hazards from future eruptions: U.S. Geological Survey Professional Paper 1022-C, 17 p.
- Johnson, A. M., 1970, *Physical processes in geology*: San Francisco, California, Freeman, Cooper and Company, 577 p.
- Kamb, W. B., 1959, Ice petrofabric observations from Blue Glacier, Washington, in relation to theory and experiment: *Journal of Geophysical Research*, v. 64, p. 1891–1904.
- Luzier, J. E., 1969, *Geology and groundwater resources of southwestern King County, Washington*: Washington Division of Water Resources Water-Supply Bulletin 28, 260 p.
- Major, J. J., 1996, Experimental studies of deposition by debris flows: Process, characteristics of deposits, and effects of pore-fluid pressure [Ph.D. dissert.]: Seattle, University of Washington, 34 p.
- Major, J. J., and Voight, B., 1986, Sedimentology and clast orientations of the 18 May 1980 southwest-flank lahars, Mount St. Helens, Washington: *Journal of Sedimentary Petrology*, v. 56, p. 691–705.
- Mark, D. M., 1973, Analysis of axial orientation data, including till fabrics: *Geological Society of America Bulletin*, v. 84, p. 1369–1374.
- Mark, D. M., 1974, On the interpretation of till fabrics: *Geology*, v. 2, p. 101–104.
- Matthes, F. E., 1914, *Mount Rainier and its glaciers*, Mount Rainier National Park, Washington: Washington, D.C., U.S. Department of the Interior, 48 p.
- Mills, H. H., 1984, Clast orientation in Mount St. Helens debris-flow deposits, North Fork Toutle River, Washington: *Journal of Sedimentary Petrology*, v. 54, p. 626–634.
- Middleton, G. V., 1970, Experimental studies related to problems of flysch sedimentation, *in Lajoie, J., ed., Flysch sedimentology in North America*: Toronto, Ontario, Business and Economic Science Ltd., p. 253–272.
- Mullineaux, D. R., 1965a, Geologic map of the Auburn quadrangle, King and Pierce counties, Washington: U.S. Geological Survey Quadrangle Map GQ-406, scale 1:24 000.
- Mullineaux, D. R., 1965b, Geologic map of the Black Diamond quadrangle, King and Pierce counties, Washington: U.S. Geological Survey Quadrangle Map GQ-407, scale 1:24 000.
- Mullineaux, D. R., 1974, Pumice and other pyroclastic deposits in Mount Rainier National Park, Washington: U.S. Geological Survey Bulletin 1326, 83 p.
- Mullineaux, D. R., 1986, Summary of pre-1980 tephra-fall deposits erupted from Mount St. Helens, Washington State, U.S.A.: *Bulletin of Volcanology*, v. 48, p. 17–26.
- Neall, V. E., and Alloway, B. V., 1986, Quaternary volcanoclastics and volcanic hazards in Taranaki: *New Zealand Geological Survey Record* 12, p. 101–137.
- Ostercamp, W. R., Hupp, C. R., and Blodgett, J. C., 1986, Debris-flow activity and associated hazards on Mount Shasta, Northern California: U.S. Geological Survey Professional Paper 1396-C, 21 p.
- Palmer, B. A., Alloway, B. V., and Neall, V. E., 1991, Volcanic-debris-avalanche deposits in New Zealand—Lithofacies organization in unconfined, wet-avalanche flows, *in Smith, G. A., and Fisher, R. V., eds., Sedimentation in volcanic settings: Society for Sedimentary Geology (SEPM) Special Publication* 45, p. 89–98.
- Phillips, C. J., and Davies, T. R. H., 1991, Determining rheological parameters of debris flow material: *Geomorphology*, v. 4, p. 101–110.
- Pierson, T. C., 1985, Initiation and flow behavior of the 1980 Pine Creek and Muddy River lahars, Mount St. Helens, Washington: *Geological Society of America Bulletin*, v. 96, p. 1056–1069.
- Pierson T. C., and Scott, K. M., 1985, Downstream dilution of a lahar: Transition from debris flow to hyperconcentrated streamflow: *Water Resources Research*, v. 21, p. 1511–1524.
- Richardson, K., 1982, *Rivers, form and process in alluvial channels*: London and New York, Methuen, 358 p.
- Russell, I. C., 1898, *Glaciers of Mount Rainier, with a paper on the rocks of Mount Rainier by G. O. Smith*: U.S. Geological Survey 18th Annual Report, Part 2, p. 349–423.
- Schuster, R. L., and Crandell, D. R., 1984, Catastrophic debris avalanches from volcanoes, *in Proceedings IV, Symposium on Landslides, Volume 1*: Toronto, Ontario, p. 567–572.
- Scott, K. M., 1988, Origins, behavior, and sedimentology of lahars and lahar-runout flows in the Toutle-Cowlitz River system: U.S. Geological Survey Professional Paper 1447-A, 74 p.
- Scott, K. M., and Vallance, J. W., 1995, Debris-flow, debris-avalanche, and flood hazards at and downstream from Mount Rainier, Washington: U.S. Geological Survey Hydrologic Investigations Atlas HA-729, 9 p.
- Scott, K. M., Pringle, P. P., and Vallance, J. W., 1992, Sedimentology, behavior, and hazards of debris flows at Mount Rainier, Washington: U.S. Geological Survey Open-File Report 90-385, 106 p.
- Scott, K. M., Vallance, J. W., and Pringle, P. P., 1995, Sedimentology, behavior, and hazards of debris flows at Mount Rainier, Washington: U.S. Geological Survey Professional Paper 1547, 56 p.
- Siebert, L., Glicken, H., and Ui, T., 1987, Volcanic hazards from Bezymianny- and Bandai-type eruptions: *Bulletin of Volcanology*, v. 49, p. 435–459.
- Sparks, R. S. J., 1976, Grain-size variations in ignimbrites and implications for the transport of pyroclastic flows: *Sedimentology*, v. 23, p. 147–188.
- Stuiver, M., and Reimer, P. J., 1993, Extended <sup>14</sup>C data base and revised CALIB <sup>14</sup>C age calibration program: *Radiocarbon*, v. 35, p. 215–230.
- Ui, T., 1989, Discrimination between debris avalanches and other volcanoclastic deposits, *in Latter, J. H., ed., Volcanic hazards*: Berlin, Springer-Verlag, p. 201–209.
- Vallance, J. W., 1994a, Postglacial lahars and potential volcanic hazards in the White Salmon river drainage basin on the southwest flank of Mount Adams volcano, Washington: U.S. Geological Survey Open-File Report 94-440, 51 p.
- Vallance, J. W., 1994b, Experimental and field studies related to the behavior of granular mass flows and the characteristics of their deposits [Ph.D. dissert.]: Houghton, Michigan Technological University, 197 p.
- Varnes, D. J., 1978, Slope movement types and processes, *in Schuster, R. L., and Krizek, R. J., eds., Landslides—Analysis and control*: National Academy of Sciences, Washington, D.C.: U.S. Transportation Research Board Special Report 176, p. 11–35.
- Wolman, M. G., 1954, A method of sampling coarse river-bed material: *Eos (Transactions, American Geophysical Union)*, v. 35, p. 951–956.
- Yamaguchi, D. K., 1983, New tree-ring dates for recent eruptions of Mount St. Helens: *Quaternary Research*, v. 20, p. 246–250.

MANUSCRIPT RECEIVED BY THE SOCIETY JUNE 8, 1995

REVISED MANUSCRIPT RECEIVED APRIL 9, 1996

MANUSCRIPT ACCEPTED MAY 14, 1996